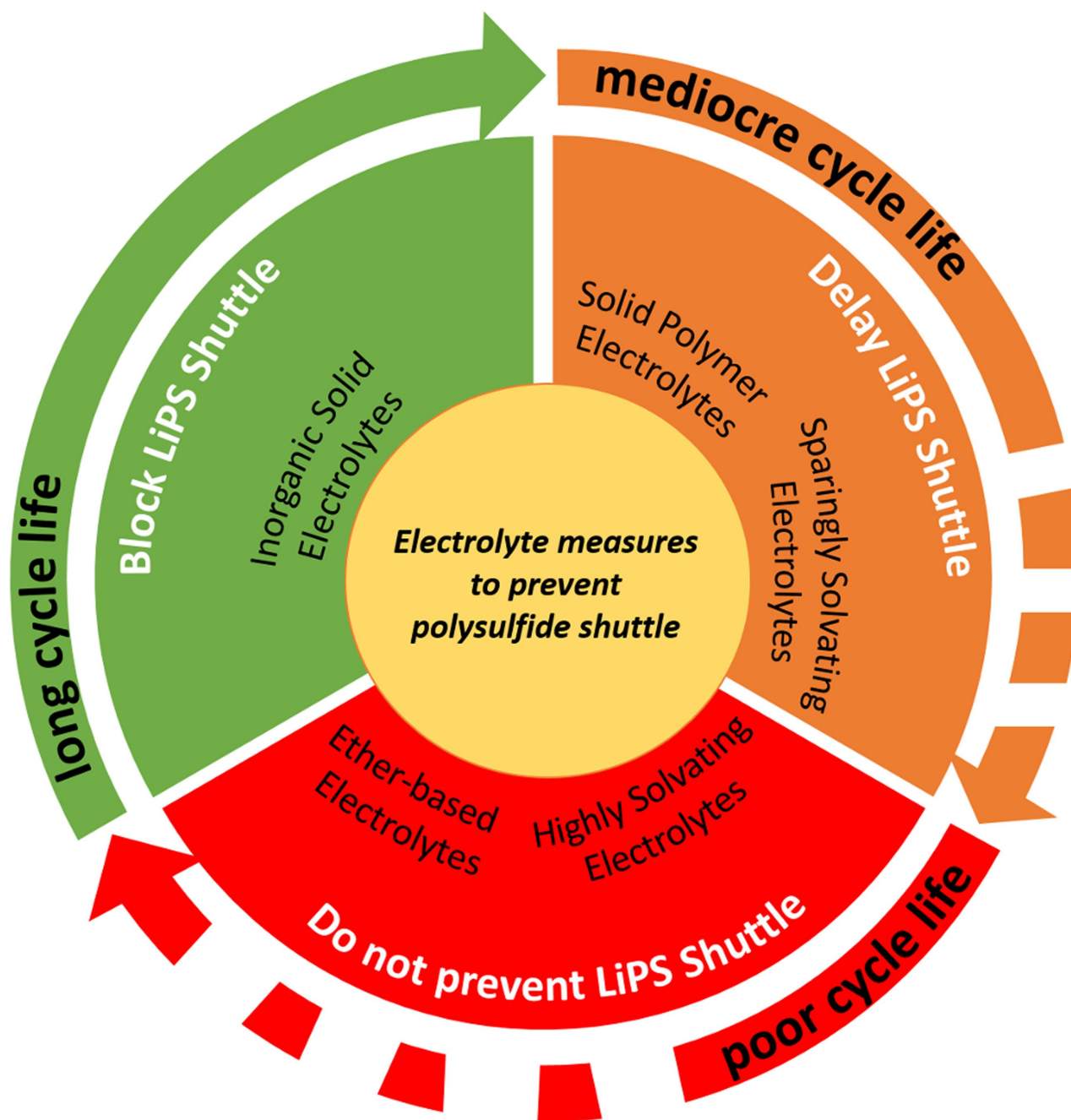


Special
Collection

Electrolyte Measures to Prevent Polysulfide Shuttle in Lithium-Sulfur Batteries

Graziano Di Donato^{+, [a, b, c]} Tugce Ates^{+, [b, c]} Henry Adenusi,^[d] Alberto Varzi,^{*, [b, c]}
Maria Assunta Navarra,^{*, [a]} and Stefano Passerini^{*, [b, c]}



Lithium-sulfur (Li–S) batteries are recognized as one of the most promising technologies with the potential to become the next-generation batteries. However, to ensure Li–S batteries reach commercialization, complex challenges remain, among which the tailoring of an appropriate electrolyte is the most important. This review discusses the role of electrolytes in Li–S

batteries, focusing on the main issues and solutions for the shuttle mechanism of polysulfides and the instability of the interface with lithium metal. Herein, we present a background on Li–S chemistry followed by the state-of-the-art electrolytes highlighting the different strategies undertaken with liquid and solid electrolytes.

1. Introduction

While the last century was unquestionably dominated by energy generation from fossil fuels, the 21st century seems devoted to the energy transition towards more sustainable sources. The increase of social and political awareness regarding global warming as well as national interests in reaching energy supply independence, including evaluations regarding the non-renewability of fossil fuels, are driving technological innovations towards the efficient use of sustainable energy sources. Lithium-ion batteries (LIBs) are becoming the leading energy storage technology for mobile applications including electric vehicles (EVs) for transportation.^[1] However, the integration of intermittent renewable energy sources within the electricity grid, the continuous technological progress resulting in more powerful portable devices on the market, including the rapid growth of EVs, increasingly push the demand for batteries with higher energy densities, lower cost, and longer lifespan. The relatively slow progress on improving the specific (gravimetric) capacity of positive electrode materials (cathodes) and volumetric capacity of negative electrode materials (anodes) are the bottlenecks limiting LIB's performance. Consequently, the research has been progressively oriented towards batteries that overcome the limitation of intercalation chemistries.^[2,3] In this framework, lithium-sulfur batteries (LSBs), employing a sulfur-based cathode in combination with a lithium metal anode, is very promising due to the high theoretical specific capacity (1,675 mAhg⁻¹) of sulfur and the resulting specific

energy (2,500 Whkg⁻¹). Additionally, LSBs have reached a certain maturity, which may enable the next step beyond the Li-ion configuration in the short to medium term. Furthermore, sulfur has the edge because it is non-toxic, abundant with a homogeneous spread thus it is a low-cost material ($\approx 180 \text{ USD ton}^{-1}$)^[4] when compared with elements widely used today in commercial LIBs like cobalt ($\approx 80,000 \text{ USD ton}^{-1}$), which is also listed in the European *Critical Raw Materials* chart,^[5] and nickel ($\approx 35,000 \text{ USD ton}^{-1}$).

Despite the first reports which appeared in the 1960s,^[6–8] LSBs have not been developed to the performance level required for practical applications. The chemistry inside LSBs does not only carry the above-mentioned advantages, but also a few outstanding issues.

Firstly, the electronic and ionic insulating characteristic of sulfur (about $10^{-30} \text{ Scm}^{-1}$) requires the use of extensive ionic and electronic conductive matrices. These result in a low fraction of active material present in the positive electrode, which decrease the overall cell gravimetric and volumetric energy densities.^[9] In addition, the low electronic and ionic conductivity of its end-discharge product Li₂S (about $10^{-14} \text{ Scm}^{-1}$) can passivate the cathode with an insulation barrier preventing the full reduction of the loaded sulfur.^[10,11]

Secondly, the difference in density of sulfur (2.06 g cm^{-3}) and lithium sulfide (1.67 g cm^{-3}) implies a severe volumetric expansion/shrinkage during discharge/charge cycles. The mechanical stress acting on the cathode architecture results in discontinuities of the ionic and electronic pathways, leading to serious irreversible capacity fade.^[12,13]

Thirdly, when typical organic liquid electrolytes are used, soluble polysulfide intermediates (LiPSs) form during cycling. These migrate from the cathode to the anode, under a gradient concentration, where they react with metallic lithium to form shorter polysulfides, and vice versa, activating the so-called “shuttle effect” (see Section 1.1).

Finally, the non-uniform stripping/deposition of lithium results in dendritic and mossy structures on the anode surface. These deposits, increasing the electrode surface area led to the continuous formation of the solid-electrolyte interphase (SEI), which results in an increase of polarization and in the formation of “dead lithium”. Additionally, dendrites may potentially pierce the separator resulting in short-circuits, which can trigger the thermal runaway phenomenon.^[14,15]

While in the last decades significant advances have been made with a deeper understanding of the lithium-sulfur chemistry, further research efforts are required to bridge the gap between laboratory results and practical applications (Figure 1). The most important requirements for the commerci-

[a] G. Di Donato,[†] Prof. Dr. M. A. Navarra
 Department of Chemistry
 Sapienza University of Rome
 Piazzale Aldo Moro 5, 00185 Rome, Italy
 E-mail: mariassunta.navarra@uniroma1.it

[b] G. Di Donato,[†] Dr. T. Ates,[†] Dr. A. Varzi, Prof. Dr. S. Passerini
 Helmholtz Institute Ulm (HIU)
 Helmholtzstrasse 11, 89081 Ulm, Germany

[c] G. Di Donato,[†] Dr. T. Ates,[†] Dr. A. Varzi, Prof. Dr. S. Passerini
 Karlsruhe Institute of Technology (KIT)
 P.O. Box 3640, 76021 Karlsruhe, Germany
 E-mail: alberto.varzi@kit.edu
 stefano.passerini@kit.edu

[d] Dr. H. Adenusi
 Hong Kong Quantum AI Lab (HKQAI)
 17 Science Park West Avenue, Hong Kong 999077, China

[[†]] These authors contributed equally to this work.

 An invited contribution to a Special Collection dedicated to Lithium–Sulfur Batteries

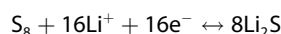
 © 2022 The Authors. Batteries & Supercaps published by Wiley-VCH GmbH. This is an open access article under the terms of the Creative Commons Attribution License, which permits use, distribution and reproduction in any medium, provided the original work is properly cited.

alization of LSBs refer to the positive electrode, i.e., high sulfur content (≥ 70 wt%), high areal sulfur loadings (≥ 5 mg cm $^{-2}$) and high areal capacities (≥ 6 mAh cm $^{-2}$) but also involve the electrolyte. In particular, the electrolyte/sulfur (E/S) ratio should be lower than 4 μ L mg $^{-1}$.^[16]

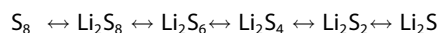
To fulfil this latter requirement, (as well as to address the above-mentioned non-uniform lithium plating and polysulfide shuttle issues), the development of practical LSBs requires engineering of the interfaces and interphases granting protection of the lithium anode,^[17–19] as well as the cathode's composition and architecture.^[9] These can only be achieved via the improvement of the separator and the electrolyte's design.

1.1. The shuttle of polysulfides

In contrast to the intercalation “rocking-chair” mechanism of the LIBs, LSBs are characterized by a conversion chemistry. As the most stable form at room temperature and atmospheric pressure of elemental sulfur is the orthorhombic crystal structure arranged in octasulfur crown, the overall electrochemical reaction is:



This electrochemical process is composed of a multi-step reaction that involves the formation of intermediate lithium polysulfides Li $_2$ S $_x$ ($2 \leq x \leq 8$). During cell discharge the sulfur rings open and lithiation occurs forming progressively shortened chain length polysulfides until one lithium sulfide is gradually re-oxidated in the following charge process resulting in a reversible cycle (Figure 2a). In the first instance, it is well-accepted that the process can be defined by the formation of four main LiPSs:



Several in operando studies have presented a more complex reaction pathway that involves the formation of polysulfide anions and radicals.^[21,22] The polysulfides undergo a variety of disproportionation and exchange reactions in solution that in addition to the solvent-dependence of these processes, does not permit a clear identification of a unique reaction pathway.^[23] The complexity of this framework is further complicated considering that the electrochemical process is not the only one involved in the reaction mechanism but also chemical processes, like precipitation and dissolution, participate in the alteration of the reaction equilibria and kinetics by changing the electrochemical potentials of the other species involved.^[24]



Graziano Di Donato received his MSc Degree in Industrial Chemistry at Sapienza University of Rome. During his academic career he approached the field of electrochemical energy storage. He is enrolled as PhD Student in Chemical Sciences. His current research interests solid state batteries, focusing especially on lithium sulfur technology.



Tugce Ates received her MSc degree in Chemistry and Management at the Ulm University. She completed her PhD in 2021 in the group of Prof Passerini at the Helmholtz Institute Ulm (HIU), affiliated with the Karlsruhe Institute of Technology (KIT). Recently, she is serving as a postdoc focusing on the development of solid-state batteries.



Henry Adenusi is a Postdoctoral Fellow at the Hong Kong Quantum AI Lab, The Centre of Machine Learning for Energy Materials and Devices at The University of Hong Kong. His research focuses on the computational study of electrolytes for lithium batteries as well as new electrochemical systems.



Alberto Varzi studied Chemistry of Materials at University of Bologna (Italy) and received a PhD in 2013 from the Ulm University and the Center for Solar Energy and Hydrogen Research Baden-Württemberg (ZSW). After a postdoctoral period at MEET battery research centre – University of Muenster, in 2014 he joined the Helmholtz-Institute Ulm (HIU) of the Karlsruhe Institute for Technology (KIT). Since 2021 he is Principal Investigator and leads the group “Electrochemistry of Materials and Interfaces”. His current research interests span from solid state to aqueous batteries, including beyond-Li systems.



Maria Assunta Navarra is researcher in Physical Chemistry at Sapienza University of Rome, Department of Chemistry, where she is leading the group of Electrochemistry and Nanotechnologies for Advanced Materials (ENAM). Her research is focused on functional materials for energy storage and conversion, both electrodes and electrolytes for batteries, fuel cells and electrolyzers.



Stefano Passerini is Professor at the Karlsruhe Institute of Technology, Helmholtz Institute Ulm. His research activities are focused on electrochemical energy storage with special focus on improving the sustainability of high-energy batteries.

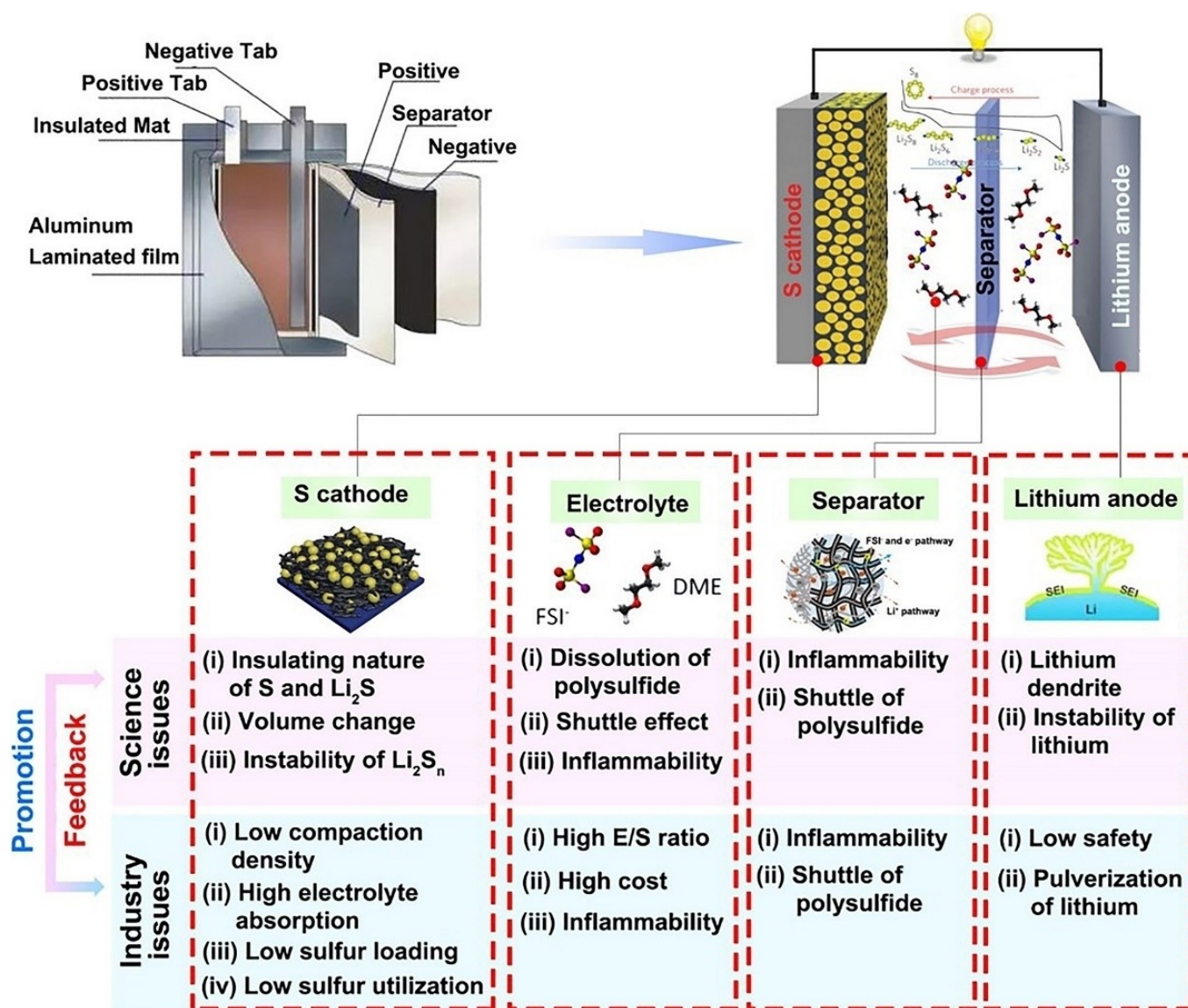


Figure 1. The correlated issues between industrial applications and scientific research for LSBs. Reproduced with permission from Ref. [20]. Copyright (2018) Zhengzhou University.

In the charging phase the accumulation in solution of an increasing number of high-order polysulfides, before the solid-phase sulfur precipitation, create a concentration gradient forcing a diffusion mechanism of these species from the cathode to the anode surface where they are reduced by the small potential of the lithium metal. Consequently, the high concentration of reduced species at the anode involves a back-flux of these species to the cathode. These LiPSs crossover generating an internal parasite current called the “polysulfide shuttle” (Figure 2b) that leads to detrimental consequences with a direct impact on the energy density and lifespan of the batteries:

(i) The diffusion of the long-chain polysulfides to the anode, where they are reduced to short-chain, leads to an incomplete charging caused by the parasitic current generated and as a result a low Coulombic Efficiency.

- (ii) In the extreme case, $\text{Li}_2\text{S}_2/\text{Li}_2\text{S}$ deposition may occur on the Li electrode resulting in the direct reaction of the two electrode materials and in a low sulfur utilization with irreversible capacity loss.
- (iii) The $\text{Li}_2\text{S}_2/\text{Li}_2\text{S}$ deposition may also accelerate the lithium dendrite growth generating a rough surface.
- (iv) A serious self-discharge of the cell occurs caused by the continuous loss of the active material.

Currently there are two main approaches for suppressing the shuttle effect:^[25] (i) preventing the diffusion of polysulfide into electrolyte using porous materials to confine them,^[26–28] anchoring polysulfide on the cathode surface by chemical/physical adsorption,^[29–32] and decreasing their solubility into the electrolyte; (ii) blocking the migration pathway of polysulfide by modifying the separator^[33–35] or the inserting of interlayers.^[36]

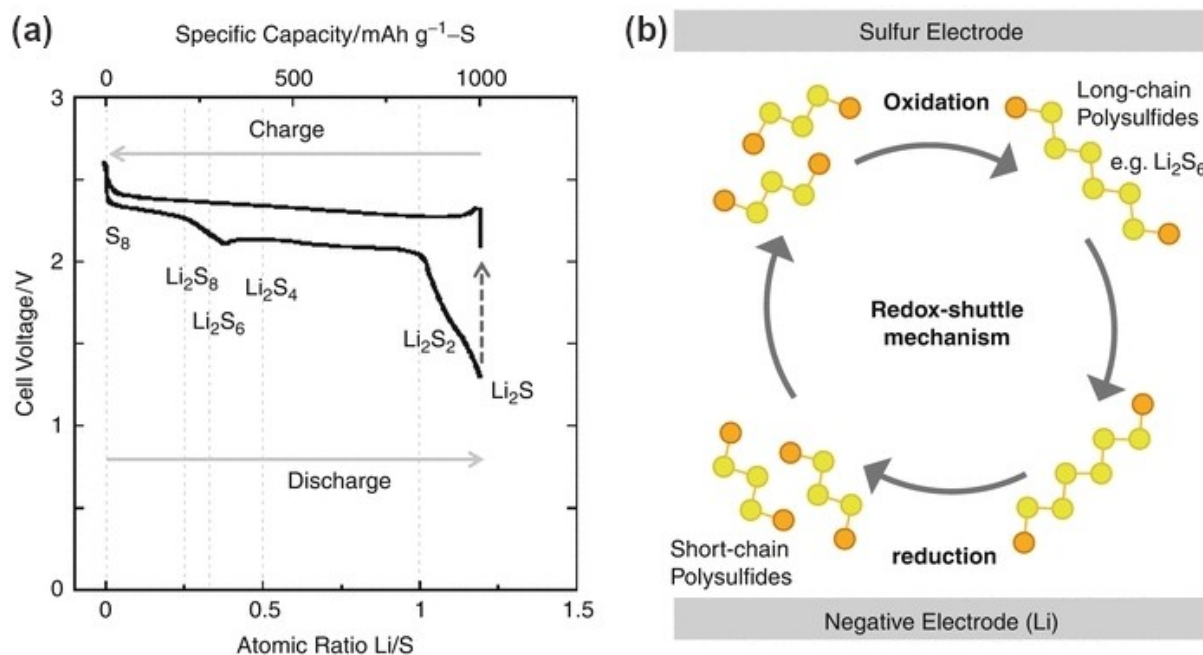


Figure 2. a) Typical voltage profile of LSBs with an organic liquid electrolyte; b) the schematic redox-shuttle mechanism. Reproduced with permission from Ref. [37].

2. Liquid Electrolytes

The electrolyte solution plays an arguably more important role in LSBs than in conventional LIBs. In the dissolution-deposition chemistry of liquid electrochemical lithium-sulfur systems, the electrolyte not only serves as a conductor for positively charged ions transport but also participates in the conversion reactions. Usually, the optimization of the electrolyte solution is achieved through the choice of solvents, salts and eventually additives to satisfy key parameters like high ionic conductivity, low viscosity, compatibility with electrodes and a suitable electrochemical stability window. For LSBs, the choice must also be driven by specific solvent properties that can influence the stability of polysulfides and so the chemical equilibrium among the dissolved species. Currently, the principal solvent dictator suggested for the evaluation of the stability of LiPSs is the donor number (DN) that is defined as a quantitative measure of Lewis basicity. Since Li^+ is a Hard Acid and polysulfide anions are Soft Bases, according to the Hard Soft Acid Base (HSAB) Theory this ion couple is not stable. As evidenced by He et al., high-DN solvents preferentially stabilize long-chain polysulfides and radicals, whereas the Li ions solvated in low-DN solvents facilitate the medium and short chain polysulfides speciation.^[38] The traditional carbonate-based electrolytes used for LIBs are reported to be unsuitable for LSBs because of the rapid irreversible reaction of the polysulfides species with the most electrophilic carbon of the solvent via nucleophilic addition or substitution.^[39] This involves the formation of thio-carbonates species which interrupts the cascade of discharging reactions, resulting in poor battery performance. As a result, Yim and co-workers suggest that more electrophilic solvents than carbonates such as esters, aldehydes, ketones, and anhydride-type should be avoided for LSBs. Historically, ethers like 1,3-dioxolane

(DOL), 1,2-dimethoxyethane (DME), diethylene glycol dimethyl ether (DEGDME),^[40,41] tetraethylene glycol dimethyl ether (TEGDME)^[42,43] and their mixtures, are conventional solvents for liquid electrolytes in LSBs due to their ability to initiate the solid-liquid transition in the sulfur cathode, and the relatively good chemical stability towards highly nucleophilic LiPS intermediates. In particular, the binary mixture of DOL and DME has emerged as the preferred choice for LSBs as DOL has a positive effect on the flexible SEI-formation, and DME with its stronger solvation capability for LiPSs provides higher reaction kinetics.

Similarly, the traditional lithium salts used in conventional LIBs, such as lithium hexafluorophosphate (LiPF_6) and lithium tetrafluoroborate (LiBF_4) are not suitable for LSBs since they can react with polysulfides.^[44] Although Lithium bis(fluorosulfonyl)imide (LiFSI) is often used, lithium bis(trifluoromethanesulfonyl)imide (LiTFSI) is currently dominating the literature for LSBs. Its popularity could be ascribed mostly to its high thermal stability, high ionic conductivity, good dissociation ability and good compatibility in ether solvents and polysulfides.^[45]

Currently, 1.0 M LiTFSI dissolved in DOL/DME (1:1 v/v) solvents mixture, with the addition of a specific amount (typically 1 wt%–5 wt%) of lithium nitrate (LiNO_3) as additive can be considered the standard liquid electrolyte benchmark for LSBs. However, the generally used ether-based electrolyte solution requires many solvent molecules to achieve a full depth of lithiation and so an excess amount of electrolyte is required, especially for high loading sulfur electrodes. Although progress has been made over the years to improve cycling stability and rate performances, usually these results have been achieved using large amounts of electrolyte. In such conditions, the electrolyte consumption is alleviated, and the lifespan of

the cell “doped”, as well as the decreasing of mass transfer/transport resistance results in high capacity and rapid rate capability.^[46] Recently, lean-electrolyte-conditions have emerged as a feasible approach to achieve practical high energy density LSBs. The amount of electrolyte used reduces the competitiveness of LSBs compared to LIBs shifting the energy density away from the goal of $\geq 500 \text{ Wh kg}^{-1}$ and increasing the cost.^[47,48] If on one hand the increment of dissolved LiPSs providing faster kinetics for solution-mediated redox reactions can increase the sulfur active material utilization, and thereby enhancing the specific capacity, on the other hand a high polysulfide solubility in electrolyte leads to concerns worsened when we operate with limited amount of electrolyte, especially with elevated sulfur loading.^[49] When the volume of the electrolyte drops to match practical LSBs requirements, problems related to the electrolyte solution are exacerbated. In particular, the increased sulfur concentration gradient results in a more severe shuttle of the polysulfides leading to a faster corrosion of the anode and loss of active material. Furthermore, a lower E/S ratio outcome produces a higher viscosity for the electrolyte leading to lower wettability and lower ionic conductivity and so an increased charge-transfer resistance of the cells.^[50] In addition, using low electrolyte amounts in Li–S cells generally leads to significantly lower

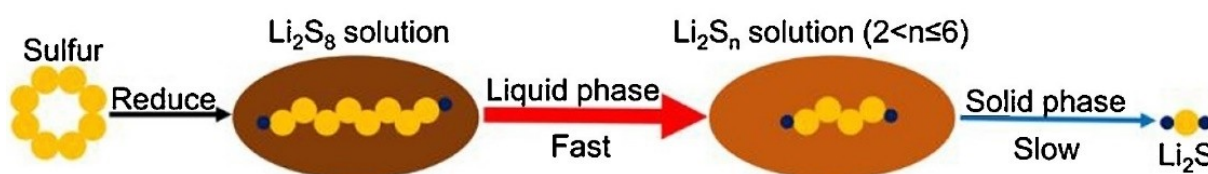
specific capacities, as well as electrolyte depletion induced by the uncontrolled growth of Li metal dendrites that react continually consuming the limited electrolyte. This can be considered as the main mechanism accountable for early Li–S cells failure. The role of the anode in the lifespan of the LSBs is less defined in coin cell laboratory-level configuration with an excess of Li and electrolyte, while it is prominent in the scale-up to pouch cell configuration.^[51]

The solubility of LiPSs and therefore the choice of the solvents in the electrolyte solution affects the reaction pathway ultimately influencing the electrochemical performance of LSBs. In a study, Shen et al. reported that when saturation is reached in the electrolyte, further sulfur conversion no longer follows an electrochemical catholyte reduction, but rather a quasi-solid mechanism. Although sulfur is reduced to solid-state LiPSs in saturated electrolytes, its further electrochemical conversion is hindered by the finite LiPSs solubility therefore the cell does not reach its maximum theoretical capacity (Figure 3).^[52]

In recent years, two main strategies based on two opposite philosophies have been developed for polysulfide shuttle management:

- (i) sparingly Solvating Electrolyte solutions (SSEs).
- (ii) highly Solvating Electrolyte solutions (HSEs).

Before saturation:



After saturation:

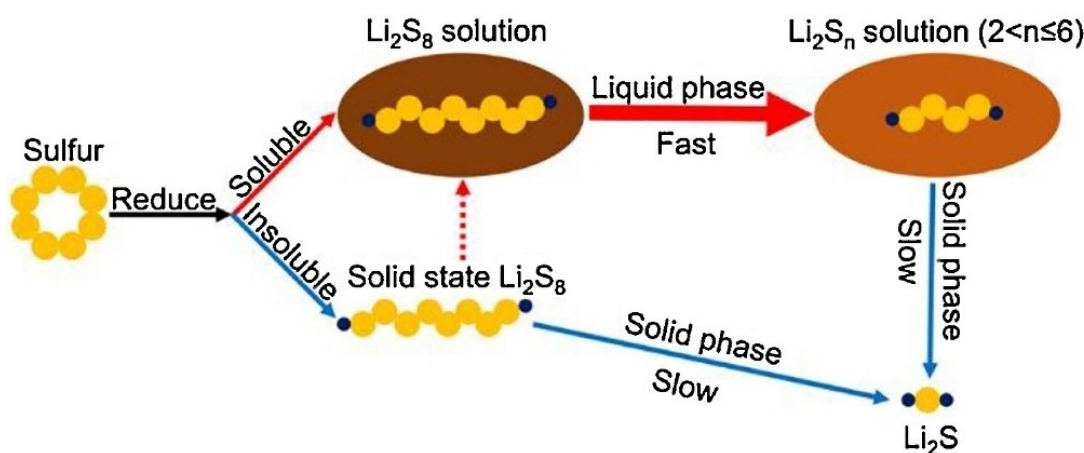


Figure 3. A schematic illustration of the differences in the reaction pathway in unsaturated and saturated LiPSs organic electrolytes. Reproduced with permission from Ref. [52]. Copyright (2017) Published by Elsevier Ltd.

2.1. Sparingly solvating electrolytes

The concept of SSEs is based on the suppression of the LiPSs solubility using solvents with weak solvating power. On the market there are already successful commercialized applications based on precipitation-dissolution mechanism in which intermediates are only sparingly soluble such as lean-acid and sodium iron chloride batteries (ZEBRA).^[53] The reduction of LiPSs solubility mitigates the shuttle effect and the anode corrosion improving the LSBs cyclability. In addition, the transformation of sulfur conversion from the dissolution-precipitation to quasi-solid pathway decouple the dependence of the sulfur electrochemical reactions on the electrolyte amount, allowing the cell to operate in lean-electrolyte conditions. However, the quasi-solid interconversion leads to sluggish kinetics, that limits rate performances, and low sulfur utilization. Nevertheless, LSBs based on the solid-solid conversion still face problems such as instability of Li metal anode. In this regard, ionic liquids (ILs) and solvate ionic liquids (SILs), hydrofluoroethers (HFEs) and highly concentrated electrolytes (HCEs) were widely investigated.

Ionic liquids and solvate ionic liquids – ILs have attracted attention in the field of energy storage systems as alternative solvents for electrolytes principally for the capability to combine favorable physicochemical properties, such as lower flammability and a negligible volatility, with good electrochemical features such as reasonably high ionic conductivities and wide electrochemical windows. Regarding LSBs, ILs offer advantages since they are typically composed of weak Lewis acidic cations and weak Lewis basic anions thus, they can suppress the LiPSs solubility.^[54,55] Watanabe's group performed a series of milestone studies.^[55–59] They found that the structure of anions influences the electrolyte properties. Fixing the IL cation and changing the anion resulted in better capacities when the latter was bulky and fluorinated due to lower DN caused by the delocalization of the charge (Figure 4a). Keeping the same IL anion and changing the cation, the capacity decreases in relatively good agreement with the order of the lithium transport properties (Figure 4b).^[56]

However, the relatively slow Li^+ diffusion processes and the low ionic transference numbers in these highly viscous IL-based electrolytes represent a shortcoming for the electrochemical performance of LSBs and their successful operation with high

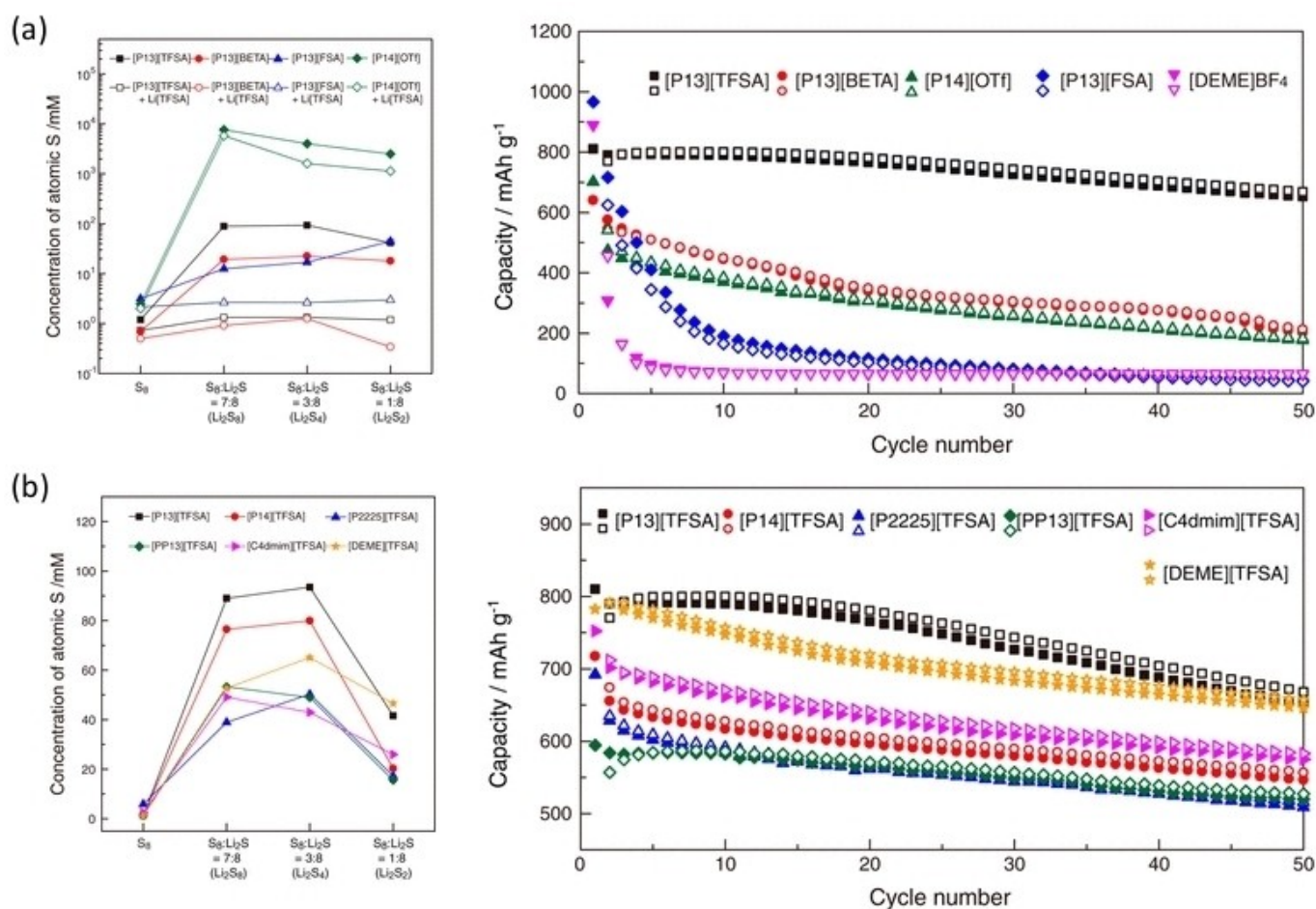


Figure 4. a) Saturation concentrations of sulfur and polysulfides in pyrrolidinium ILs with different anions and cycling performance; b) saturation concentrations of sulfur and polysulfides in TFSA ILs with different cations and cycling performance. Reproduced (adapted) with permission from Ref. [56]. Copyright (2013) American Chemical Society.

current density. For this reason, a class of so-called “Solvate Ionic Liquids” was proposed. Instead of binary mixtures of aprotic ILs and Li salts, a coordinating solvent and salt that give rise to a complex with very similar properties to ILs were investigated as alternative electrolyte (Figure 5a).^[60] The premise of this approach is that the presence of a low-viscous organic solvent could on one hand, improve the Li^+ conductivity and the transference number. While on the other hand, the formation of solvent-salt chelate complexes can weaken the intrinsic donor ability of ether solvent where excess glymes (potentially capable of solvating LiPSs) doesn't exist.

Glymes structures, and in particular long chains glymes such as TEGDME (G4), due to the presence of solvating oxygen atoms, are recognized to be favorable for the solvation of lithium ions (Figure 5b).^[61] Ueno *et al.* studying different equimolar mixtures of Li salts and glymes noticed that the dissolution of LiPSs was significantly suppressed in $[\text{Li}(\text{G4})][\text{BET}]$. The solvate IL $[\text{Li}(\text{G4})][\text{BET}]$ was found to be electrochemically stable in the Li-S cell allowing a stable operation with a capacity of 600–700 mAh g^{-1} and a Coulombic Efficiency of 98.5% over 100 cycles.^[57]

Hydrofluoroethers – HFEs is a class of solvent who, thanks to their versatility, gained a huge interest as electrolytes co-solvent for several battery configurations including lithium-ion, lithium-sulfur, lithium-air, and sodium-ion batteries.^[62] Firstly, the non-flammability and the good electrochemical stability of the HFEs improve the safety limits and expand the electrochemical window of the systems in which they are used. Moreover, lithium anode corrosion can be significantly reduced with the presence of chemically inert HFEs, leading to high Coulombic Efficiency. But their popularity increased especially for LSBs, because alongside these advantages, their low solvation strength can suppress the shuttle effect of LiPSs.

Starting from the SILs approach, Dokko *et al.* confirmed that when $[\text{Li}(\text{G4})][\text{TFSA}]$ was diluted with 1,1,2,2-tetrafluoroethyl 2,2,3,3-tetrafluoropropyl ether (TTE), improved electrochemical behaviors were obtained. Firstly, the diffusion coefficient increases with increasing molar ratio of HFE. Secondly, the LiPSs

was further suppressed (Figure 6a) resulting in high Coulombic Efficiencies and good cycle stability (Figure 6b).^[59] Similar results were obtained by Cuisinier *et al.* using an acetonitrile-salt complex $[(\text{ACN})_2\text{-LiTFSI}]$ with TTE as co-solvent. These results indicate that the combination of low polarity of the HFE with the steric hindrance of the chelating oxygen by fluorine does not participate in the solvation mechanism of lithium salts (and of lithium polysulfides too) and so, it does not break the glyme-Li complex, enhancing the power density of the LSBs.^[61]

The effect of the addition of HFEs is also visible in “simpler” solvent systems. Gu *et al.* proved that the dissolution of LiPSs can be effectively reduced by adding 1,3-(1,1,2,2-Tetrafluoroethoxy) propane (FDE) in a traditional DOL/DME mixture with 1.0 M LiTFSI as salt. In ultraviolet-visible (UV-vis) spectroscopy measurements (Figure 7a) it is evident that as the FDE amount increases in the solution, the absorbance curve of S_x^{2-} species flattens. Moreover, the HFE-added electrolytes can protect the lithium anode from corrosion. In particular, an even more compact and homogenous surface can be observed within the increment of FDE in the electrolyte (Figure 7b).^[63]

Also, Talian *et al.* observed higher areal capacity with low electrolyte amount using 1,2-(1,1,2,2-tetrafluoroethoxy)ethane (TFEE) based electrolytes compared to 1.0 M LiTFSI in DOL and TEGDME traditional electrolytes. In addition, studying the altered voltage profiles of the TFEE based electrolyte they pointed out that the origin for the shifting of the curve is the poor lithium-ion solvation ability of the fluorinated ethers.^[64]

Azimi *et al.* performed X-ray photoelectron spectroscopy (XPS) on lithium metal previously immersed in TTE solvent for 12 h, concluding that the protection on lithium is due the formation of a LiF-rich composite layer on its surface given by the reductive decomposition of fluoroether. This protective layer could serve as a physical barrier to the reactions of the LiPSs on the anode surface.^[65]

The restrained sulfur solubility and the high quality SEI given by HFEs solvents were proven to positively affect not only the shuttle and Li corrosion by LiPSs, but also the self-discharge of LSBs.^[66,67] However, a certain sulfur dissolution still

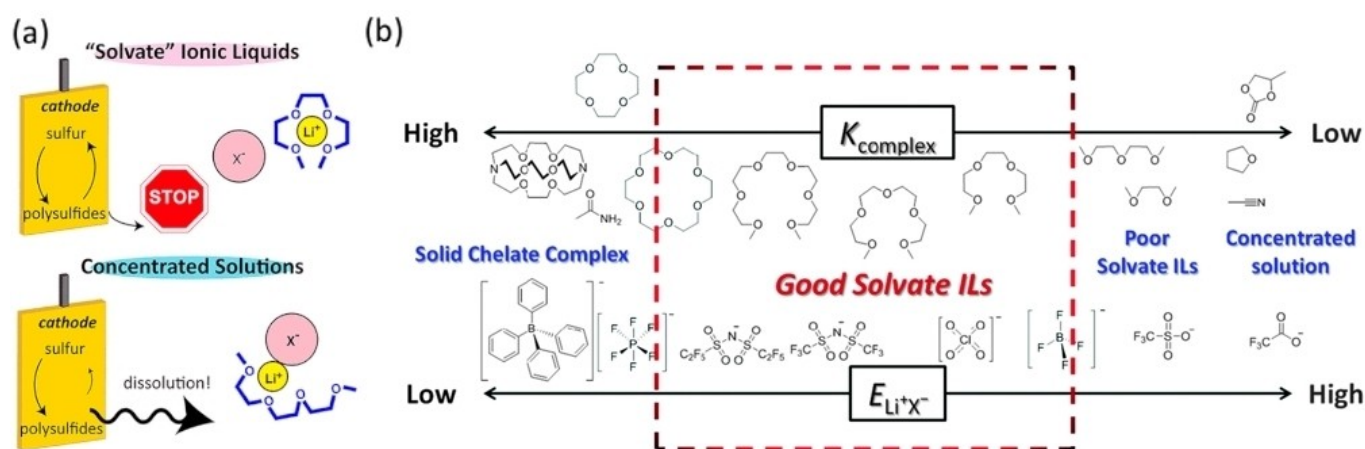


Figure 5. a) Schematic concept of Solvate Ionic Liquids. Reproduced with permission from Ref. [57]. Copyright (2013) American Chemical Society; b) model of classification of Solvate Ionic Liquids. Reproduced with permission from Ref. [58]. Copyright (2014) Royal Society of Chemistry.

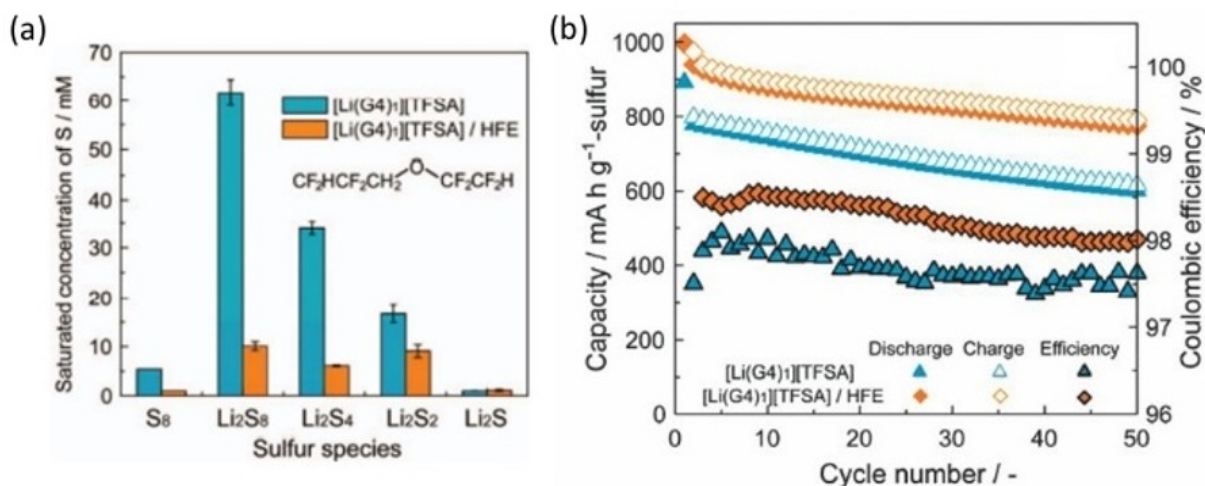


Figure 6. Comparison between [Li(G4)]TFSA and [Li(G4)]TFSA/HFE in terms of a) sulfur and polysulfides solubility and b) cycling performance. Reproduced with permission from Ref. [59]. Copyright (2013) The Electrochemical Society.

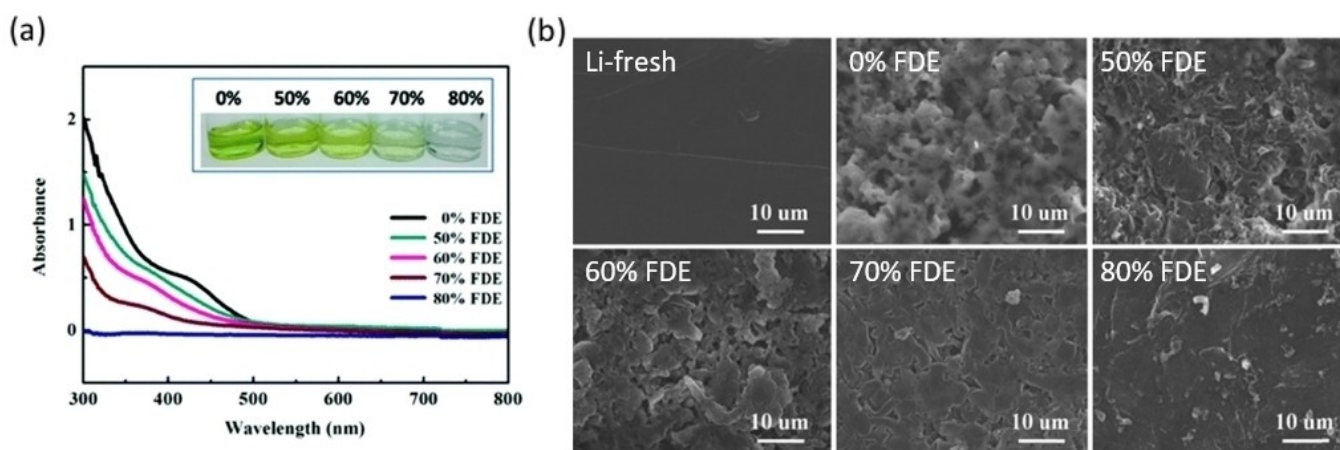


Figure 7. Comparison of electrolytes with different amount of FDE added in DOL/DME solution for a) UV-vis spectroscopy measurements and b) for scanning electron microscopy (SEM) images of Li anode before (Li-fresh) and after 20 cycles. Reproduced with permission from Ref. [63]. Copyright (2016) The Royal Society of Chemistry.

exists, using 1,1,2,2-Tetrafluoroethyl 2,2,2-Trifluoroethyl Ether (TTFTE) as co-solvent in (1.0 M LiTFSI) DOL/DME electrolyte demonstrated that a part of the active species loss in the period of resting can be restored, showing better reversibility than the electrolyte without this partially fluorinated ether.^[67]

Recently, Lu et al. proposed a balanced ternary electrolyte of DEMETFSI IL/TTE/DOL and LiTFSI as salt, able to synergistically pair the lower viscosity, better SEI-construction and weaker LiPSs dissolution of the IL/TTE binary mixture with the higher utilization of active material of the IL/DOL mixture.^[68]

Highly concentrated electrolytes – For conventional non-aqueous organic electrolytes, the salt concentration is usually limited in a range of 1.0–2.0 M.^[69] At higher concentrations, the higher viscosity and the reduced ionic conductivity of the electrolyte increases polarization of the electrodes. In this range of concentration only a small fraction of solvent is involved in the solvation of Li⁺, while most of the solvent molecules are free to further dissociate other lithium compounds (Figure 8a),

such as LiPSs. As the concentration of salt increases, the interaction between cations and anions becomes stronger forming anions coordinated to a single solvated Li⁺ cation, “contact ion pairs” (CIPs) and anions coordinated to two or more Li⁺ cations, “aggregates” (AGGs) (Figure 8b). This means a lower number of free solvent molecules, and thus, a lower solvating power available for LiPSs. In fact, the solubility of lithium polysulfide (ξ) from the sulfur cathode will be controlled by the concentration of lithium salt (C) present in the electrolyte by the common ion effect according to the following relation:^[70]

$$\frac{\xi}{\xi_0} = \left(\frac{2\xi_0}{C}\right)^2$$

where (ξ_0) is the LiPSs solubility when no lithium ion is present in the electrolyte. In their work, Shein et al. reported that in concentrated electrolytes the reduced solubility of lithium

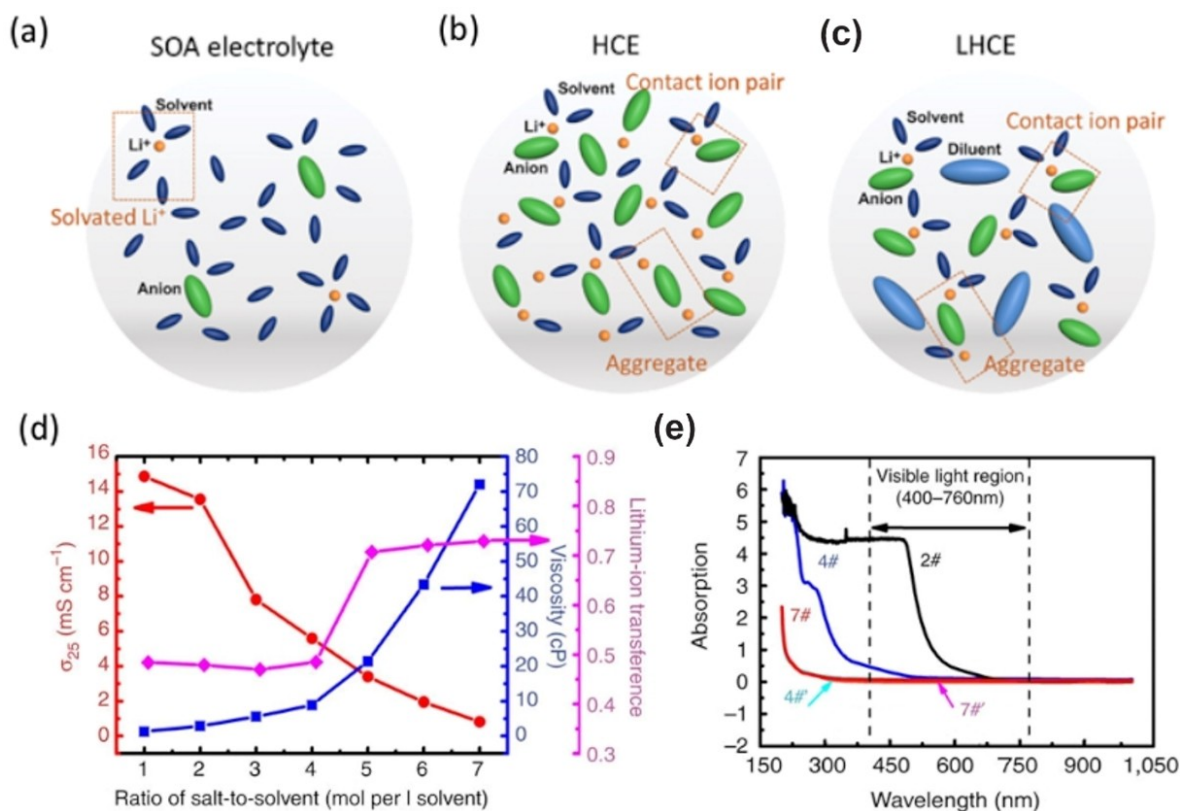


Figure 8. Electrolyte structures of a) conventional electrolyte, b) HCE and c) LHCE. Reproduced with permission from Ref. [71]. Copyright (2021) The Author(s). Published on behalf of The Electrochemical Society by IOP. d) Viscosity, ionic conductivity and Li-ion transference number of the DOL/DME with different amounts of LiTFSI; e) UV-vis spectroscopy measurements of the solution with different concentrations of LiTFSI after 18 days. Reproduced with permission from Ref. [69]. Copyright (2013) Nature Publishing Group.

polysulfides and the decreased diffusion coefficient result in a lower amount of overcharge and, thus, in better Coulombic Efficiencies.^[70]

In 2013 Suo *et al.* first introduced the concept of Solvent-in-Salt (SIS), systems in which the amount of salt is above 3.5 mol L⁻¹. Studying different concentration of LiTFSI in DOL/DME (1:1 v/v) they pointed out that although the increasing of salt concentration is reflected in higher viscosity and, thus, in lower ionic conductivities, a Li⁺ transference of 0.73 can be reached in the 7 M electrolyte because of the strong solvation interactions (Figure 8d). Moreover, the inhibition of the LiPSs solubility (Figure 8e) effectively protect the metallic lithium anode providing a Coulombic Efficiency of nearly 100% and 74% of Capacity Retention (0.2 C) after 100 cycles for the most concentrated solution.^[69]

However, the high viscosity and the poor wettability of the electrodes with this type of electrolyte are not favorable for practical application. To avoid the drawbacks, in the last years the concept of localized high-concentration electrolyte (LHCE) has emerged. Diluting HCE with cosolvent with non-solvating power, such as HFEs, the overall salt concentration is reduced but the highly concentrated salt-solvent clusters are preserved (Figure 8c).^[71]

Lastly, since the salt represents about 90% of the electrolyte, a five times increment of its amount would mean a 400% increase in cost, hindering an industrial scale up.^[72]

2.2. Highly solvating electrolytes

As an alternative strategy towards practical LSBs, HSEs were suggested to promote the polysulfides dissolution to minimize the electrolyte amount and reach at least the target of 500 Wh kg⁻¹ of energy. As pointed out by Gupta *et al.*, to reach this target E/S ratio of 5 $\mu\text{L mg}^{-1}$ (or lower) is theoretically required but considering a more practical sulfur utilization this amount would be reduced to at least 2 $\mu\text{L mg}^{-1}$. This E/S ratio value corresponds to a 1.6 M Li₂S₆ concentration in the electrolyte, amount that exceeds the maximum polysulfides solubility in traditional DOL/DME system at room temperature.^[73] The focus shifts to high-DN solvents owing to their strong Lewis basicity that preferentially dissociate alkali metal salts solvating their Lewis acidic cations and, thus, stabilizing polysulfides with lower charge density like long-chain PS and the tri-sulfur radical.

In 2019 Gupta *et al.* compared N,N-dimethylacetamide (DMA), dimethyl sulfoxide (DMSO) and 1-methylimidazole (MeIm), with a DN of 28, 30 and 47, respectively. As shown in Figure 9(a) these three solvents can effectively dissolve 1.5 M concentration of Li₂S₆ at room temperature, while in the DOL/DME binary mixtures the presence of undissolved sulfur species is evident. Furthermore, the resultant blue solutions in DMA and DMSO suggest the presence of S₃^{•-} species. The latter is present in larger amount in the DMA solvent, as shown by the

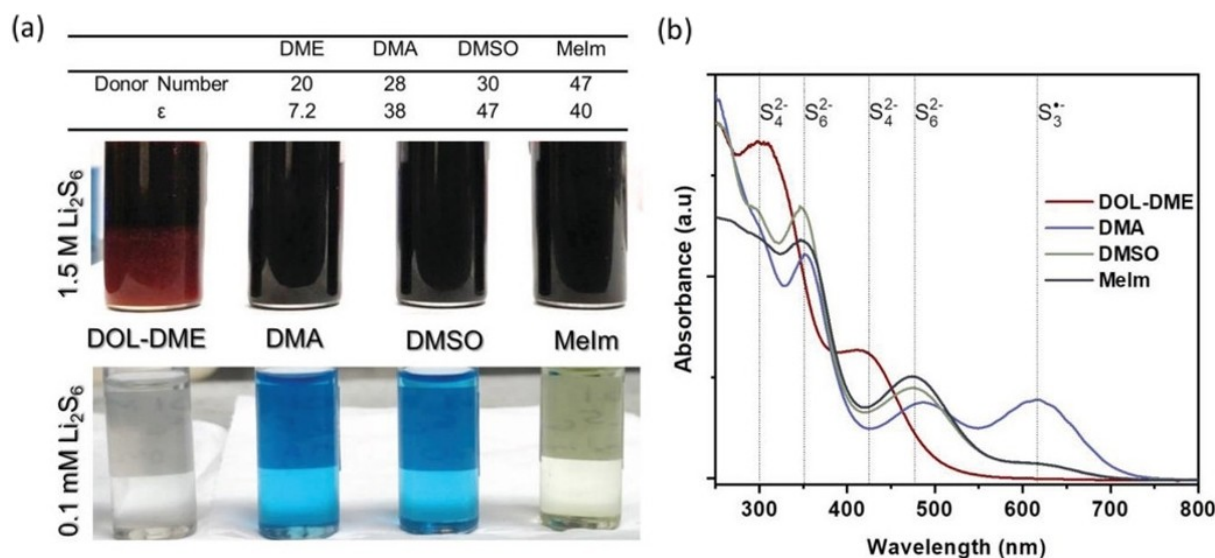


Figure 9. a) Optical images of different nominal Li_2S_6 concentrations dissolved at room temperature in solvents with different donor number and dielectric constant (ϵ); b) UV-vis spectra for 0.25 M Li_2S_6 in different solvents. Reproduced with permission from Ref. [73]. Copyright (2018) WILEY-VCH Verlag GmbH & Co. KGaA, Weinheim.

UV-vis spectroscopy measurements (Figure 9b), and the differences in the intensity peaks of the various species confirms that the reaction pathway for LSBs is solvent-dependent. Overall, high DN solvents are able to activate a different reaction route which engages the sulfur radical $\text{S}_3^{\bullet-}$.^[73–75]

The presence of $\text{S}_3^{\bullet-}$ species acting like a redox mediator can facilitate a full utilization of sulfur active material and decrease the overpotential of Li_2S oxidation, forming Li_2S deposits in the shape of large particles, instead of films. This allows the electrode to circumvent passivation by insulating Li_2S and to retain its conductive surface to enable stable redox reactions (Figure 10a).^[75]

This solution-mediated precipitation was also confirmed by Baek et al., who proposed the 1,3-dimethyl-2-imidazolidinone (DMI) as a new high DN solvent for LSBs (Figure 10b and 10c). This is because stabilizing the carbonyl group of ethylene carbonate (EC), through the replacement of the two oxygen atoms with nitrogen, the typical nucleophilic attack of sulfide anions versus the carbonyl group can be avoided. The impact on the performance in lean-electrolyte conditions of the DMI is reported in Figure 11(a and b). Using 5 μL of electrolyte per mg of sulfur, although in the first 30 cycles the DOL/DME- LiNO_3 0.2 M cell showed a good stability and higher capacities with respect to the DMI- LiNO_3 0.5 M, during prolonged cycling a rapid decay of the performance is shown caused by the insufficient amount of the electrolyte. In contrast the DMI-based cell retains 59.6% of its original capacity after 80 cycles with high Coulombic Efficiencies.^[74]

Despite these advantages, additional efforts must be undertaken with respect to long-term stability performances. A higher polysulfides solubility is linked to a more severe LiPSs shuttle phenomenon. Furthermore, high-DN solvents are more reactive to the lithium metal anode as shown in Figure 12,

where the lithium metal collected after 1 cycle worsens with the increment of the donor number of the solvent.^[73]

2.3. Lithium metal anode protection

Lithium metal is currently regarded as a preferred electrode material for the anode of next generation high-performance energy storage systems mainly due to its performances such as low gravimetric density (0.59 g cm^{-3}), high theoretical specific capacity ($3,860 \text{ mAh g}^{-1}$) and good negative redox potential (-3.040 V vs. SHE).^[76] Despite these properties, the utilization of such a reactive metal in different electrochemical systems such as batteries is limited by issues primarily related to the non-uniform stripping/deposition of the lithium and the presence of side reactions resulting in short lifespan of the cell. Therefore, the enhancement of the interfacial stability with Li-metal anode plays a key role to address the trade-off between the energy density and long-term cyclability commercially needed for LSBs. The use of reactive solvents coupled with mobile LiPSs represents the greatest barrier to effectively protect the lithium metal anode with stable passivating surface films. While most of the attempts in the last years has focused on the improvement of the sulfur cathode and on the optimization of the electrolyte solution, recently it has become clear that the bottleneck of further development of practical Li-S technology is the rapid degradation of lithium metal anodes with cycling. Different strategies for lithium metal protection have been reported in the literature, such as electrolyte additives, artificial SEI and solid-state electrolyte (discussed in the following chapter) however, the presence of polysulfides in LSBs chemistry makes this harder to regulate than in LIBs.

The low lithium reduction potential causes the irreversible decomposition of the components of the electrolyte. As a

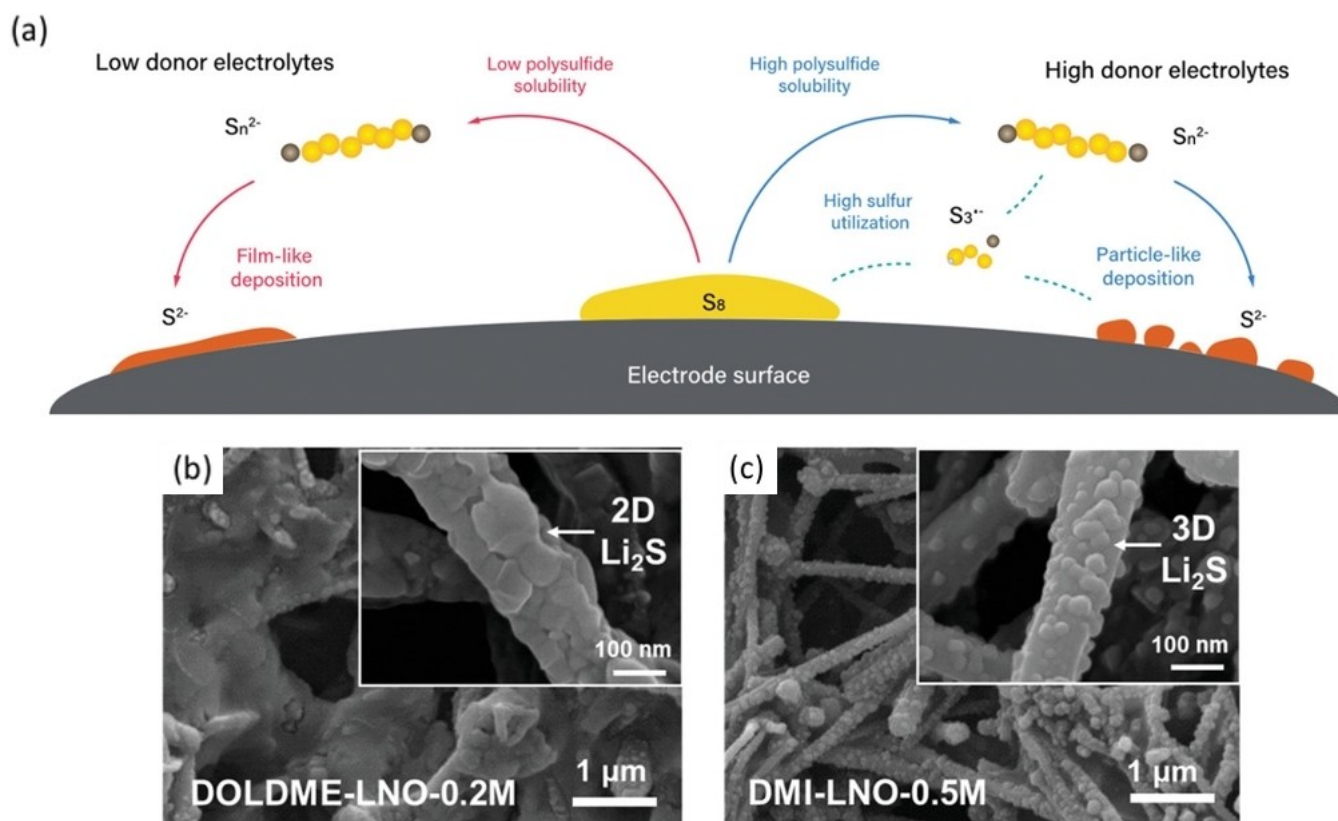


Figure 10. a) Schematic illustration of the lithiation process for low-DN and high-DN electrolytes in LSBs. Reproduced with permission from Ref. [75]. Copyright (2020) WILEY-VCH Verlag GmbH & Co. KGaA, Weinheim. b) SEM of Li_2S deposition in DOL:DME- LiNO_3 electrolyte; c) SEM of Li_2S deposition in DMI- LiNO_3 electrolyte. Reproduced with permission from Ref. [74]. Copyright (2020) WILEY-VCH Verlag GmbH & Co. KGaA, Weinheim.

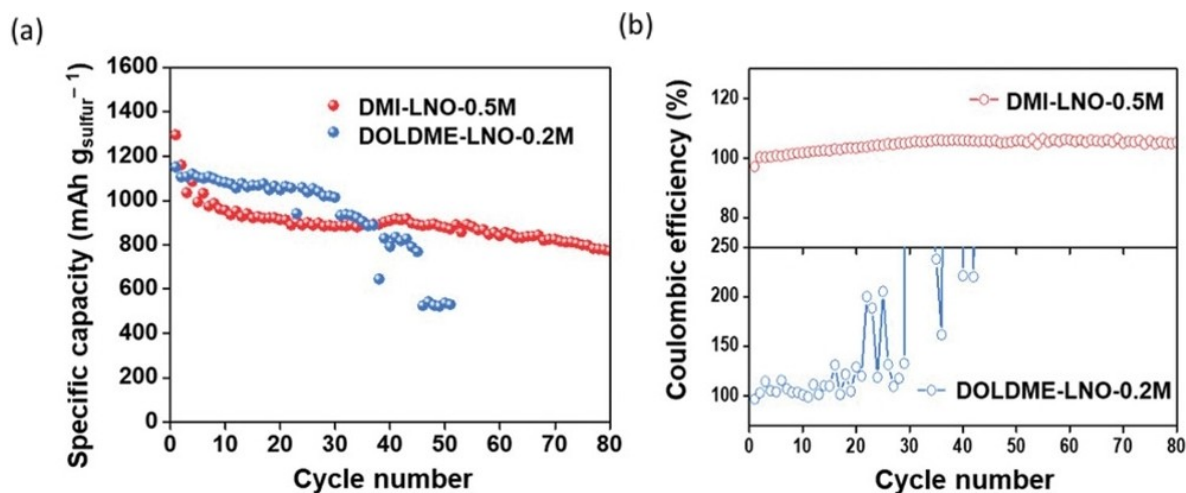


Figure 11. Comparison between DOL/DME- LiNO_3 and DMI- LiNO_3 in terms of a) cycling performance at 0.03 C and b) Coulombic Efficiency. Reproduced with permission from Ref. [74]. Copyright (2020) WILEY-VCH Verlag GmbH & Co. KGaA, Weinheim.

result, formation of the SEI on the anode surface occurs in the first cycles of the cell. Although its formation leads to sacrificing a part of the capacity, it is now well-known that this passivation layer is fundamental for the cycle-life of the system, limiting further side-reactions between the anode and the electrolyte, allowing ionic mobility through it as well as promoting uniform

metal deposition by regulating the solid-state ion flux.^[77] The uneven stripping of lithium ion from the anode surface, and its subsequent uneven deposition result in dendrites growth of the lithium. This phenomenon is one of the most challenging for the wide scale commercialization of systems which use lithium metal. As the dendrites grow, they can pierce the

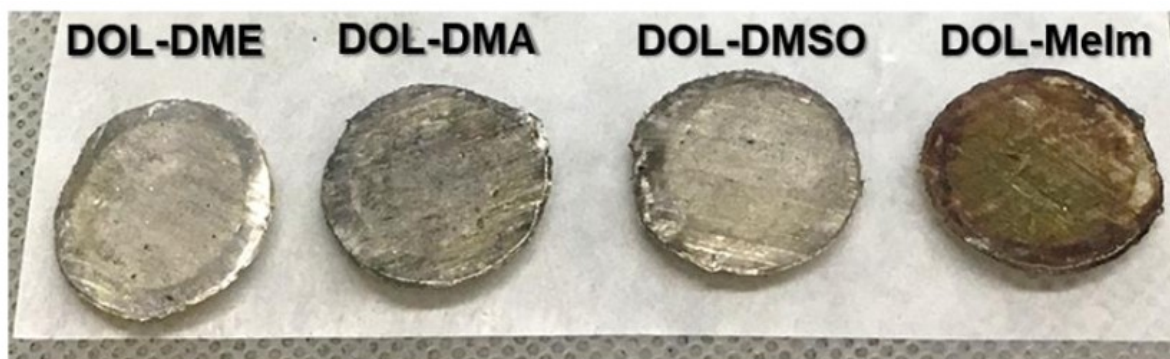


Figure 12. Lithium metal anode collected after 1 cycle in different electrolyte solutions. Reproduced with permission from Ref. [73]. Copyright (2018) WILEY-VCH Verlag GmbH & Co. KGaA, Weinheim.

separator until they are physically in contact with the cathode. The consequent short circuit can bring potential risks and safety concerns for the utilization of the device by the user. For these reasons, the chemical composition, the morphology as well as the growth are all crucial parameters affecting the stability of the SEI and, thus, the cyclability of the cell. In fact, the eventual fracturing of the fragile passivation layer during battery cycling exposes fresh lithium to continuously consume electrolyte leading to an even thicker SEI hence increasing the resistance of the cell as well as promoting the needle-like dendrites growth. In LSBs the scenario is further complicated by the presence (in the electrolyte solution) of polysulfides which participate in the composition of the SEI through their irreversible decomposition.

Although studies are limited, it is noteworthy to state that the formation of a SEI on the cathode, (CEI, cathode electrode interphase) that is able to prevent the direct contact of sulfur with the electrolyte solution and to facilitate the de-solvation of the Li ions before they react with sulfur can stabilize LSBs cycling.^[78] The porosity of the sulfur host and the sulfur loading appears to be the primary cause of variations in CEI formation mechanisms and stability. In particular, when sulfur is confined in microporous carbons a closed protective CEI layer can be formed.^[79] Chen *et al.* established that if the sulfur content is too high, the CEI could not tolerate the stress caused by the large volume variation of S_8 - Li_2S , concluding that the CEI strategy is effective only when a proper sulfur loading is used.^[80] Moreover, Markevich *et al.* confirmed that also the composition of the electrolyte solution is important for the realization of “quasi-solid-state reactions” of sulfur with Li ions in the pores of activated carbon matrices.^[81]

The strategies for the improvement of lithium metal anode should consider both the regulation of the stripping-deposition process and the prevention of lithium corrosion from side reactions, but the SEI in LSBs is expected with an additional function: to selectively block LiPSs from interacting with the lithium metal anode.^[82]

Additives – Though the ether-based electrolyte can provide high ionic conductivity and good interface contact with electrodes, the issues originating from the dissolution of

intermediate polysulfides make it necessary to add suitable additives to protect the lithium metal anode.^[83]

The additives including an N–O bond in their structure, in which the $LiNO_3$ salt is the most important, have represented a real breakthrough in lithium metal protection for LSBs because it enhances the LSBs cycling performance.^[84] Actually, several investigations have clarified that the contribution of $LiNO_3$ and polysulfides are equally important in the formation of a SEI layer able to suppress the shuttle effect.^[85,86] The synergetic effect of the $LiNO_3$ and of polysulfides lead to the formation of a robust SEI film composed of two sub layers (Figure 13a). The bottom layer is formed by the co-precipitation of reduced products from polysulfides and $LiNO_3$ (lithium sulfide and LiN_xO_y) producing a smooth and compact layer. The top layer is composed of stable oxidized products from polysulfides (lithium sulfates) which can prevent the direct contact between the polysulfides in organic electrolyte and reductive species on Li electrode.^[85] Studying the role of $LiNO_3$ in LSBs, Zhang discovered a dual function on the electrodes. Stating the above-mentioned positive effect on the lithium metal, it may be irreversibly reduced on the surface of the sulfur cathode at potentials lower than 1.6 V, affecting the reversibility of the cell.^[87,88] For this reason, deep discharge must be avoided for a long cycle life in LSBs when $LiNO_3$ is used. Even though the CEI is not widely investigated, if compared with SEI studies on the anode side, recently Ye *et al.* argued that $LiNO_3$ has two competitive effects on cathode; helping to protect the carbon matrix host but also increasing the consumption of the active sulfur. These results suggest that optimized cell performance requires an optimized amount of this additive salt.

Many researchers have been inspired to work on understanding the mechanisms of other nitrates e.g. $La(NO_3)_3$,^[89] KNO_3 ,^[90] $CsNO_3$,^[91] and NH_4NO_3 .^[92] Interestingly, Jia *et al.* obtained better performance with KNO_3 additive than with $LiNO_3$ thanks to the additional benefit effect due to the presence of an ion, like K^+ that is able to “guide” the growing lithium dendrites by electrostatic attraction and then delay their further growth.^[90] This effect is known as “self-healing electrostatic shield” (SHES), and its related mechanism whereby at low concentrations alkali cations exhibit a reduction potential lower than that of standard reduction of lithium ions.

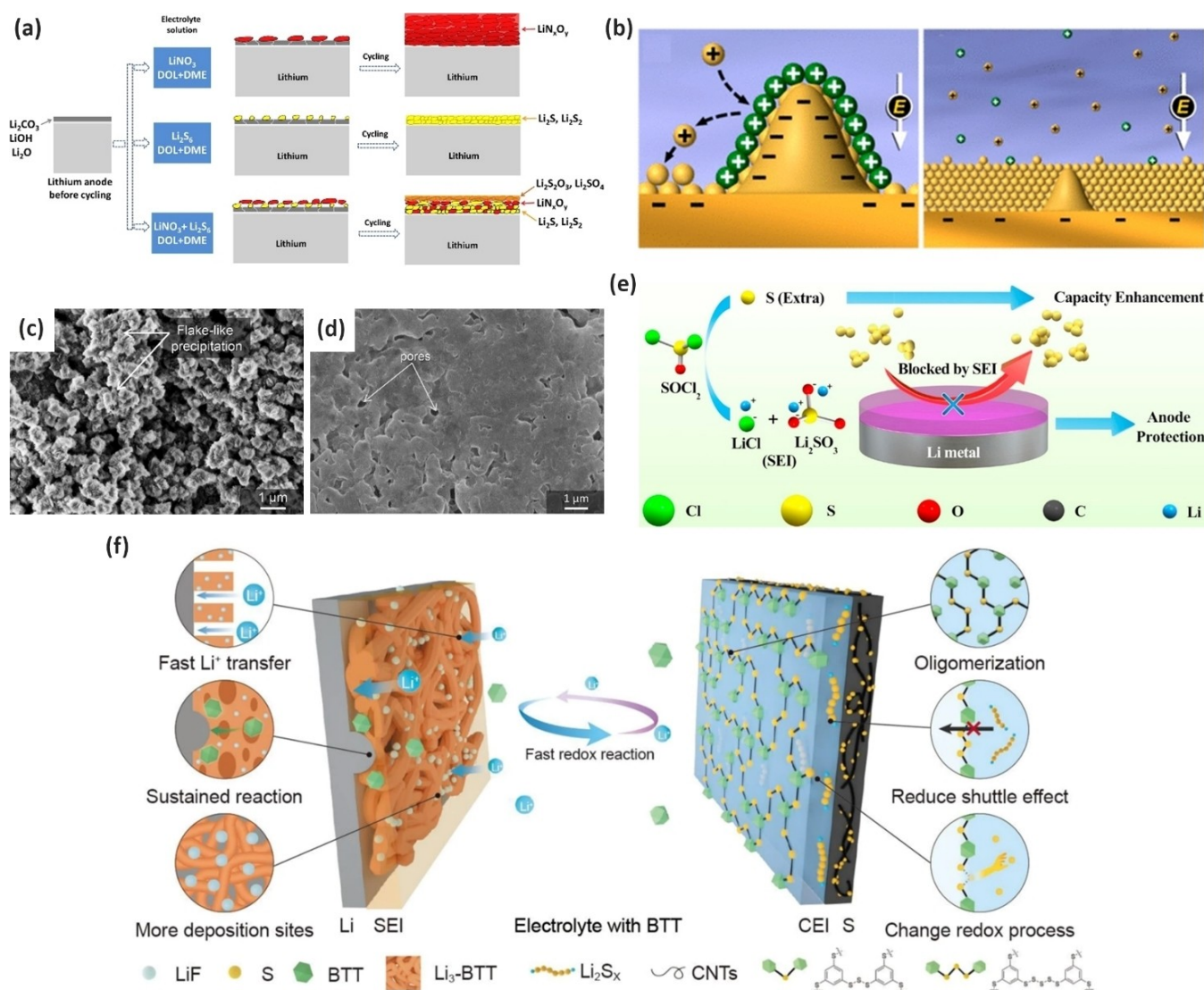


Figure 13. a) Illustration of the surface film evolution on lithium anode cycling in different electrolyte solutions. Reproduced with permission from Ref. [85]. Copyright (2013) Elsevier B.V. b) Mechanism of electrostatic shield in lithium deposition. Reproduced with permission from Ref. [93]. Copyright (2013) American Chemical Society. SEM micrograph of c) Li foil after 100 cycles in a 5 M LiTFSI, and d) Li foil after 100 cycles in a 5 M LiTFSI/0.5 M Lil electrolytes. Reproduced with permission from Ref. [99]. Copyright (2014) WILEY-VCH Verlag GmbH & Co. KGaA, Weinheim. e) SOCl_2 additive mechanism. Reproduced with permission from Ref. [102]. Copyright (2018) Published by Elsevier B.V.; f) Schematic illustration for the LSB with BTT electrolyte. Reproduced from Ref. [104]. Copyright (2021) The Author(s).

Applying a potential between these two limits, the lithium ions will start to electroplate on the anode surface, but the alkali cations do not: they will accumulate on the lithium tips forming an electrostatic shield which transform a chaotic/needle-like dendrites growth to an ordered/spheroidal growth pattern (Figure 13b).^[93]

The formation of a LiF-rich SEI film on the anode surface is beneficial to LSBs. As shown by Ni et al., the passivation layer which forms is able to inhibit the shuttle of polysulfides, avoiding the development of a $\text{Li}_2\text{S}_2/\text{Li}_2\text{S}$ insulating layer, and stabilizing the lithium anode surface.^[94] Wu et al. proved that adding an appropriate amount of Lithium difluoro(oxalato)borate (LiODFB) in the traditional 1.0 M LiTFSI DOL/DME electrolyte, promotes the formation of a LiF-rich

passivation layer on the lithium surface enabling extremely high Coulombic Efficiency and better cycle performance.^[95]

Inspired by the two previous mechanisms Li et al. attempted to combine them adding a small amount (0.01 M) of the KPF_6 additive in the 2.0 M LiTFSI, DOL/DME with 2 wt% LiNO_3 electrolyte. This approach has been demonstrated to effectively improve the stability of Li metal anode through the two synergistic effects.^[96] On one hand, electrostatic shielding from K^+ also helps to regulate a more uniform distribution of Li ions. On the other hand, the preferential decomposition of PF_6^- anion with respect to the other components of the electrolyte promotes the formation of a LiF-rich SEI.

Phosphorus pentasulfide (P_2S_5) was proposed in 2013 by Lin and co-workers.^[97] They found that in the organic electrolyte solution this compound can form soluble and non-

corrosive (versus the cell components) complexes with lithium polysulfide and lithium sulfide. The addition of P_2S_5 plays a dual role: firstly, it prevents the precipitation of Li_2S_2/Li_2S and secondly, it passivates the lithium surface with a high conductive Li_3PS_4 -rich layer that, in addition, can suppress the shuttle of polysulfides.

Another class widely studied as additives for LSBs are the iodides compounds. From the comparison of different metal iodides, LiI , MgI_2 , AlI_3 and SnI_4 , Kim and co-workers showed that electrolytes that included LiI or MgI_2 formed a stable SEI layer on the Li metal and suppressed the polysulfide shuttle reaction. This is because the viscosity of the electrolyte is appropriately increased by polymerization, and Mg ions along with Li ions are deposited on the Li metal surface to form a stable SEI.^[98] As evidenced by Wu et al. LiI undergoes oxidation at around 3 V vs. Li/Li^+ generating I^* radicals.^[99] Such radicals react with DME resulting in the formation of DME(-H) radicals which can polymerize in solution forming comb-branched polyether protective film on the cathode surface. SEM investigations show that the addition of LiI produces a very smooth Li surface (Figure 13d), while a rough surface covered with precipitates is visible in the cell without the presence of the additive (Figure 13c).

Recently indium iodide, LiI_3 , and hexadecyltriethylammonium iodide, HTOA-I, was reported as functional electrolyte additive for LSBs.^[100,101] The latter, in particular, serves multiple functions. Firstly, it permits the formation of a protective layer on the lithium anode which reduce the Li_2S_2/Li_2S deposition. Secondly, the $HTOA^+$ cation, due to its strong combination with polysulfide anions increases the difficulty of the migration to the anode. Finally, its larger size (than Li^+) is absorbed on the surface of Li anode resulting in electrostatic shielding effect, which results in a more homogeneous Li deposition.

An effective lithium protective layer was obtained using $SOCl_2$ as additive.^[102] Furthermore, the decomposition of $SOCl_2$ could produce active sulfur to offer extra capacity (Figure 13e) for the cathode in a full battery through the following reaction:



In 2017 Kim and co-workers proposed a hybrid layer formed by co-deposition of organic compounds (organosulfide, organopolysulfide) and inorganic components (Li_2S/Li_2S_2) using poly(sulfur-random-triallylamine) (PST). The presence of the organic components works like a “plasticizer” increasing its viscoelasticity producing a more flexible and stable SEI, while the inorganic components provide a Li conductive pathway and necessary mechanical hardness in the SEI layer.^[103]

Recently, 1,3,5-benzenetrithiol (BTT) additive in the electrolyte was reported to form a dual stable SEI, both on the cathode and on the anode surfaces, generated by in situ interfacial electrochemical/chemical reactions leading to high cycling stability. The SEI formed on the anode enables reversible lithium stripping/deposition. BTT also reacts with sulfur on the cathode forming on its surface an oligomer/polymer SEI which changes the redox path of sulfur and prevents the sulfur shuttle effect (Figure 13f).^[104]

Artificial SEI – Among the various strategies to enhance the stability of the Li anode, the fabrication of a protective artificial SEI on its surface is one of the most appealing for Li-metal protection. The introduction of an artificial layer can reduce the contact between the electrolyte and lithium metal, limiting electrolyte decomposition and Li-metal consumption.^[18] The protective layer should lead to a superior stability, smoothing the Li depositing pattern but, at the same time, ensuring a sufficient lithium ionic conductivity. Compared to the uncontrolled engineering of the SEI composition and morphology by adjusting electrolyte composition, the introduction of an artificial SEI a-priori has proven a practical method for Li anode protection by directly designing and constructing the liquid-solid interphase.^[105]

A Li_3N protection layer fabricated by an in-situ method showed interesting features for the protection of lithium metal such as a high Li^+ conductivity, a smooth and less resistive SEI. The protected Li anode displayed a high stability in the electrolyte compared to the bare lithium, retaining a discharge capacity of 773 mAhg^{-1} after 500 cycles with a CE above 92%.^[17]

In 2018, Cha and co-workers, demonstrated that atomic 2D layers of MoS_2 directly coated and lithiated onto the surface of Li metal can exhibit a high-capacity retention of 84% after 1,200 cycles in LSBs; this is due to a stable Li electrodeposition with dendrite formation effectively suppressed. Various phenomena that enable the electrochemical stability of the anode, such as atomically layered structure and phase-transformation behavior of the MoS_2 layer, enhance the Li^+ transport and conductivity between the electrolyte and Li metal.^[106]

Among the polymer artificial layers, the phosphorus oxynitride (LiPON) is one of the most promising due to its favorable physical properties; it is mechanically robust enough to suppress piercing from lithium dendrites. Furthermore, the LiPON-coated Li anode offers excellent electrochemical performance including a large capacity and a significantly enhanced cycle performance, even in high energy-density pouch cells.^[107]

Recently, Akhtar et al. proposed a new bifunctional inter-layer of gelatin-based fibers. Its 3D structural network, with functional polar moieties, helps to homogenize the deposition of Li, as well as hamper the shuttling effect of polysulfide during the discharge/charge processes protecting the Li anode from insoluble Li_2S_2/Li_2S deposition, which corresponds to reduce the interface impedance during cycling.^[108]

3. Solid Electrolytes

In conventional liquid electrolytes features such as diffusion, migration, solubility, and precipitation lead to irreversible capacity losses in LSBs. By transitioning from liquid electrolytes to solid electrolytes (SEs), some of these issues can be resolved to a certain extent.^[109] For instance, SEs may enable the employment of a lithium metal anode, and consequently enhance the volumetric energy density of the LSB.^[110] The main advantage of SE is that they serve not only as the electrolyte to

transfer Li ions, but they are also the separator preventing short circuit of the battery. SEs can hinder the growth of dendritic Li, and they are effective against the polysulfide shuttle as there is no way for LiPSs to dissolve and diffuse in SEs (Figure 14). SEs additionally enhance the safety aspect: no leakage and non-flammable which is ideal for next generation batteries.^[109] They provide superior thermal, chemical, and electrochemical stability, displaying good mechanical strengths with regards to conventional liquid electrolytes.

For successful use in LSBs, SEs require the following essential properties: (i) high ionic conductivity, (ii) low electronic conductivity, (iii) pre-eminent chemical stability toward lithium metal anode and sulfur cathode and (iv) a wide electrochemical stability window. Furthermore, low interfacial resistance with lithium and sulfur cathode is a necessity. What's more, non-toxic and environmentally friendly materials are also targeted.^[112]

In general, three types of SEs are utilized:

- (i) Inorganic solid-state electrolytes.
- (ii) Organic polymer electrolytes.
- (iii) Organic-inorganic hybrid electrolytes: composite polymer electrolytes.

As each of them has its specific advantages and disadvantages, though there is no ideal SE yet. In Table 1 some characteristics are summarized.

3.1. Solid polymer electrolytes

Solid polymer electrolytes (SPEs) are elastic and flexible which is also a key advantage for contact with lithium metal. Besides their superior mechanical stability, SPEs are known for their high energy density, good chemical/electrochemical stability, good thermal stability which offers improved safety, and easy as well as low-cost preparation.^[113] SPEs are in general composed of a polymer matrix with high dielectric constant and a lithium salt with lower lattice energy. Many polymers have been investigated so far, polyethylenoxide (PEO),^[114] poly(methyl methacrylate) (PMMA),^[115-117] poly(vinylidene fluoride) (PVDF)^[118,119] and poly(acrylonitrile) (PAN).^[120-122] Among them the PEO-based electrolytes are the most common in LSBs. PEO has a good stability with electrode interfaces, an excellent electrochemical stability and an acceptable Li^+ migration number.^[123] The oxyethylene (EO) group and polar groups (hydrogen, oxygen) on the PEO polymer chain can

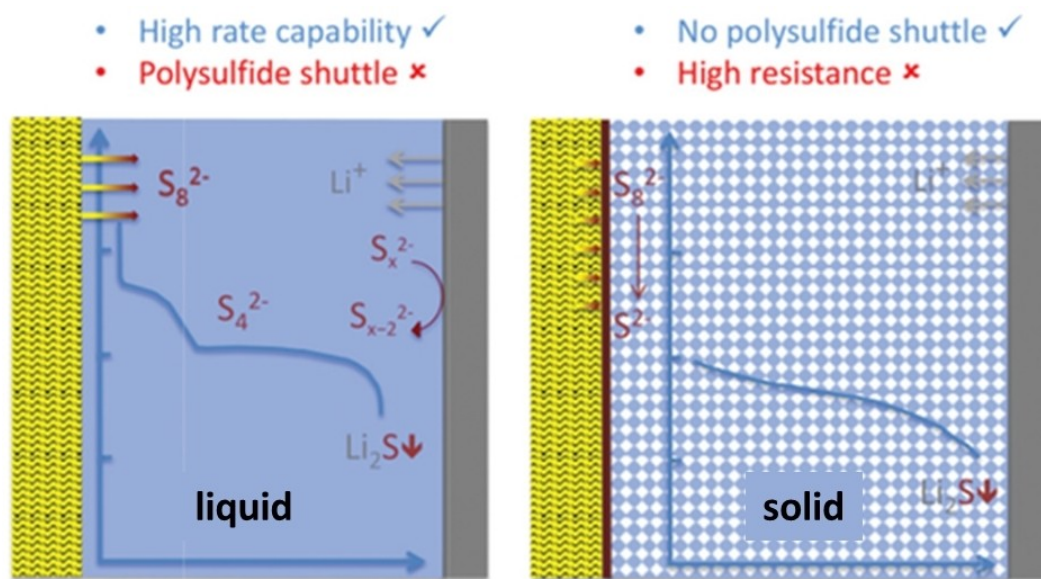


Figure 14. Schematic illustration of the liquid based LSB (left) and solid-state LSB (right). Solid electrolyte inhibits polysulfide shuttle effect. Reproduced with permission from Ref. [111]. Copyright (2020) WILEY-VCH Verlag GmbH & Co. KGaA, Weinheim.

Table 1. Different types of solid electrolytes and their advantages and disadvantages.			
Types of SEs	Classes of SEs	Advantages	Disadvantages
Inorganic solid-state electrolytes	Oxides	High ionic conductivity Good thermal and mechanical strength	High interfacial impedance
	Sulfides	High ionic conductivity Low grain boundary resistance	Sensitive towards moisture
Organic polymer electrolytes	Solid polymer electrolytes	Low interfacial impedance Stable with lithium metal Good flexibility	Low ionic conductivity Poor thermal stability
Organic-inorganic hybrid electrolytes	Composite polymer electrolytes	High ionic conductivity Low interfacial impedance	Poor thermal stability Low mechanical strength

dissolve different ionic salts, e.g., lithium salt LiX (whereas X = I, Cl, Br, BF₄, etc.). The ratio of salt/EO is important, as it determines the ionic conductivity of the polymer-salt complex. The transportation of Li ions in PEO occurs by interchain or intrachain hopping, if the salt content is too high, the Li ion motion is hindered. Furthermore, PEO suffers from poor ionic conductivity at room temperature. The motion of Li ions is quite slow at temperatures lower than the melting point of PEO (~60 °C), due to the high crystallinity of PEO at room temperature.^[113,124] On the other hand, the molten PEO at high temperatures behaves like a liquid and the shuttle effect of polysulfides is similar with ether-type electrolyte solvents.^[125,126] The cause of dissolution of polysulfides in PEO-based polymer electrolytes is the strong PEO-Li₂S_n attraction.^[127] The relatively high DN of the ethylene (EO) unit, enables the formation of long-chain polysulfides during the battery cycling causing shuttle effect in PEO electrolytes. This has been experimentally investigated by different groups. Song et al.^[125] explored the structural evolution of the polymer electrolyte via an in-situ optical microscope. During the discharge process, the color of PEO-based electrolytes changed from white into light brown because of the polysulfides dissolution into the SPE. Zaghbi's group^[128] analyzed the charge-discharge behavior of LSBs with PEO-based electrolytes via in-situ SEM imaging and UV-Vis analyses. They discovered that in the discharge process mainly S₄²⁻ polysulfides species are formed and, in the charging process S₆²⁻ is produced. The shuttle effect generates an

insulating S-rich layer on the Li metal anode, leading to increased interfacial resistance.

Although, in the past few years, researchers have focused on suppressing the shuttle effects of polysulfides and stabilizing SEI layers toward Li anodes; the focus has been on reducing the glass transition temperature and increasing the ionic conductivity of PEO at room temperature to achieve high cycle performance of Li/S cells around room temperature.^[129]

The most known SPE, PEO/LiTFSI (Lithium bis(trifluoromethanesulfonyl)imide) implemented in LSBs could barely achieve the theoretical specific capacity of sulfur at the initial cycle and underwent a fast capacity fading. PEO/LiTFSI cannot prevent the shuttle effect of LiPSs, as the SEI formed on the anode is not robust enough to retard the reaction between LiPSs and Li. However, changing the salt might help. PEO/LiFSI (Lithium bis(fluorosulfonyl)imide) for instance provides better cyclability compared to LiTFSI, as the SEI formed here is more stable on the Li anode and hinders the reaction of LiPSs and Li (Figure 15a).^[130,131] A series of lithium salts applicable to LSBs have been investigated in detail by Michele Armand's group. Besides LiTFSI and LiFSI,^[132] LiFTFSI (lithium (fluorosulfonyl)(trifluoromethanesulfonyl)imide),^[133] LiDFTFSI (lithium (difluoromethanesulfonyl) (trifluoromethanesulfonyl)imide)^[134] and LiTCM (lithium tetracyanomethanide)^[135] were the salts of interest in their studies. LiFTFSI combines the advantages of LiTFSI and LiFSI with both -SO₂CF₃ and -SO₂F functional groups. The SEI formed at the Li

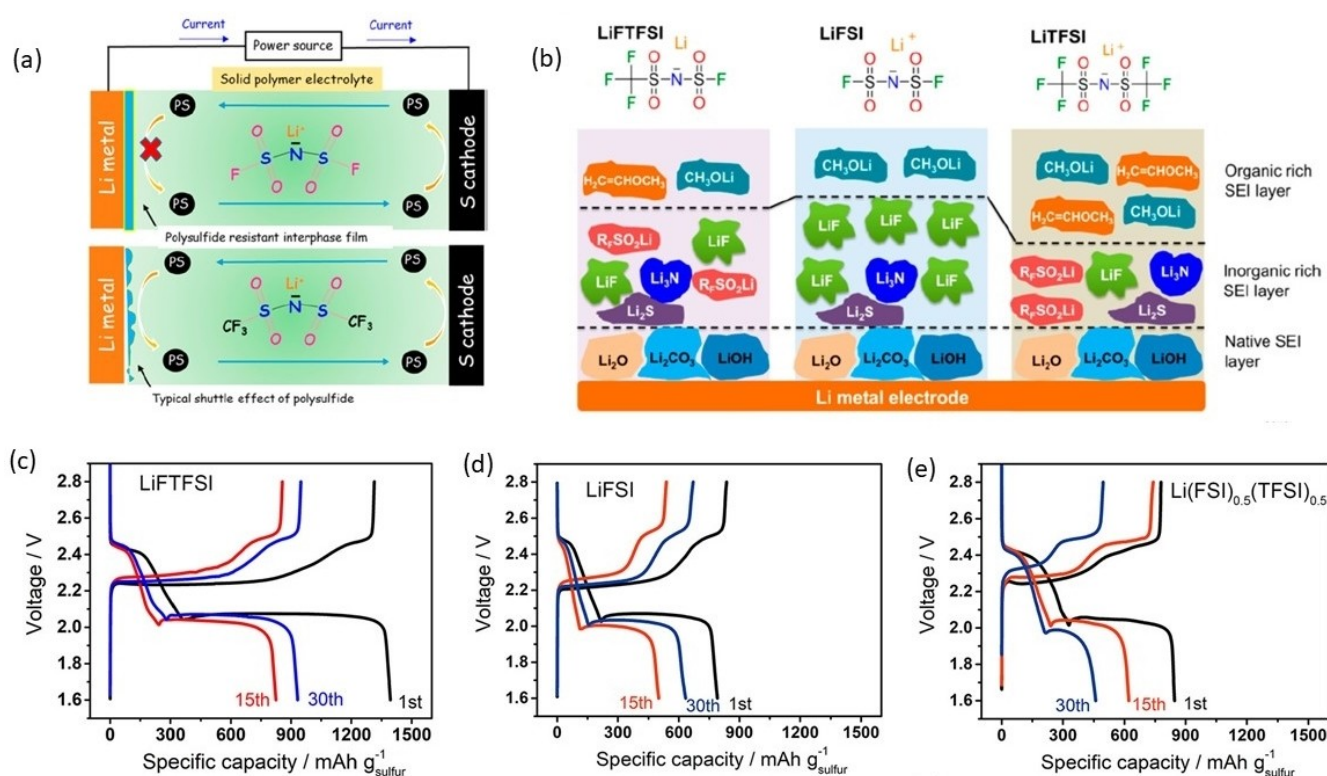


Figure 15. a) Schematic of the mechanism for Li anode protection via substitution of LiTFSI with LiFSI in PEO-based electrolyte. Reproduced with permission from Ref. [132]. Copyright (2017) American Chemical Society. b) Schematic of the SEI layer formed on a lithium electrode in LiTFSI, LiFSI and LiFTFSI; (c–e) Discharge/charge profiles of the Li–S cells using LiX/PEO (X = FTFSI, FSI, and (FSI)_{0.5}(TFSI)_{0.5}) electrolytes at 70 °C. Reproduced with permission from Ref. [132]. Copyright (2018) American Chemical Society.

and PEO/LiTFSI interface possessed an optimized organic – inorganic balance which enables a stable SEI layer with high ionic conductivity (Figure 15b). The reported LSB with PEO/LiTFSI delivered after 60 cycles is still 800 mAh g^{-1} at 0.1 C. The combination of PEO/LiDFTFSI showed that the $-\text{CF}_2\text{H}$ units of LiDFTFSI do react with PEO, thus, reducing the mobility of anion and improving the Li-ion conductivity. Moreover, the $-\text{CF}_2\text{H}$ units form a robust SEI on the Li surface and reduces the side reactions of the shuttle effect. Compared to the previous salts, LiTCM is a fluorine free salt. However, it reacts with lithium and forms a C=N network and Li_3N on the Li anode surface. Implementing PEO/LiTCM in the LSB, an initial discharge capacity of 800 mAh g^{-1} was obtained. These findings show that the lithium salts in SPEs are crucial, yet they must satisfy key requirements including high solubility and high degree of ionization in polymer hosts to achieve favorable ionic conductivities. Moreover, SEI formation with good stability and high Li conductivity is essential to enable good cyclability in LSBs.

Besides the influence of the salt, another effective strategy is to add inorganic fillers, such as oxides, sulfides and silicates to decrease the crystallinity of the PEO and increase the ionic conductivity of the polymer electrolyte. The addition of inorganic filler (such as SiO_2 , TiO_2 , AlO_2 , and ZrO_2) can adsorb polysulfides to some extent and hinder the reorganization of the chains, increasing the amorphous areas in the PEO-based SPEs, facilitating the ion transport. Additionally, the inorganic fillers can provide additional ion-conducting pathways on the fillers surface contributing to the improvement of Li-ion conductivities.^[136] For more detailed information see Section 3.3.

Another approach is to introduce a low-DN polymer, which would solve the shuttle effect by changing the reaction pathway. One interesting approach is the polysiloxilane-based SPEs, showing a conductivity of $\sim 10^{-4} \text{ S cm}^{-1}$, however, the mechanical strength of the polymers are not sufficient enough at RT.^[137,138] Also a mixed SPE consisting of a combination of several polymers as polysiloxilane, PVDF, LiTFSI in cellulose acetate was investigated, showing a relatively high ionic conductivity of $4.0 \times 10^{-4} \text{ S cm}^{-1}$.^[139]

3.2. Inorganic solid electrolytes

Inorganic solid electrolytes (ISEs) are an alternative solution to SPEs, which can effectively block the shuttle effect of polysulfides and inhibit the growth of lithium dendrites physically, due to their compact structure and exceptional mechanical properties.^[140–143] Two classes are intensively investigated, oxides and sulfides. Whereas oxides have mechanically high strengths, good thermal stability and a wide electrochemical window, some sulfides possess superior ionic conductivities higher than liquid electrolytes.

Sulfides with a high ionic conductivity up to $10^{-2} \text{ S cm}^{-1}$ have gained increasing attention.^[144] Especially, the discovery of $\text{Li}_{10}\text{GeP}_2\text{S}_{12}$ (LGPS) in 2011 has led to the development of next-generation batteries such as LSBs. The high ionic conductivity

is attributed to the fast diffusion Li ion in its crystal structure framework. However, it is unstable with lithium metal due to the reactivity of the Ge centers.^[145,146] In general, crystalline electrolytes, such as LGPS, are considered to possess higher ionic conductivities and better stability compared to their corresponding glassy systems. Typical glass-ceramic sulfides originate from the thiophosphate family $\text{Li}_2\text{S}-\text{P}_2\text{S}_5$ and $\text{Li}_2\text{S}-\text{SiS}_2$ and obtain moderate ionic conductivities in the range of 10^{-4} – $10^{-3} \text{ S cm}^{-1}$ at room temperature.^[143,147] Even though sulfides have relatively high ionic conductivities and can eliminate the polysulfide issue, they suffer from other limitations. They are not stable in ambient air, forming toxic H_2S gas.^[148] They are not chemically stable with lithium, which is why Li–In and Li–Al alloys are usually employed. Also, electrochemical decomposition of SE is observed, which tends to occur due to the unsatisfactory electrochemical stability of these materials.^[149,150]

Oxides possess a superior chemical and electrochemical stability towards lithium metal compared to their sulfidic counterparts. Garnet-type electrolytes, $\text{Li}_7\text{La}_3\text{Zr}_2\text{O}_{12}$ (LLZO) and $\text{Li}_{6.4}\text{La}_3\text{Zr}_{1.4}\text{Ta}_{0.6}\text{O}_{12}$ (LLZTO), and NASICON-type electrolyte, $\text{Li}_{1+x}\text{Al}_y\text{Ge}_{2-y}(\text{PO}_4)_3$ (LAGP), are often used in SSBs. However, oxides suffer from poor contact with electrodes causing large interfacial resistance. Even though solid-state Li/S cells are free from shuttling of LiPSs, they suffer from (i) high electrolyte/electrode interfacial impedance developed by poor interfacial contact, (ii) significant microstructural instability, (iii) dendrite formation during Li stripping/plating, and (iv) poor chemical stability.

The lithium metal/SE interface microstructure is of immense importance. The lithium dendrite growth issue at the negative electrode still persists within inorganic SEs.^[151] Tu et al.^[152] reported that the initial surface irregularities such as cracks and voids promote dendrite formation of Li metal, as the current is concentrated near the defect at the interface and causes uneven current density flow.

To inhibit these issues surface engineering is necessary. By mechanical^[153–159] and electrochemical polishing methods,^[160,161] the Li/SE interface can be smoothed, and undesired surface residues can be removed. In SSBs for instance, the surface polishing is generally performed at the SE surface facing the Li metal anode, because the surface of the pelletized SE tends to be very rough. LLZO/Li interface is significantly improved when the surface of the garnet SE is polished before. When LLZO is exposed to humid air Li_2CO_3 occurs on the surface, increasing the interfacial resistance, which can be removed by mechanical polishing. Besides mechanical surface modifications, chemical interfacial design changes are also desired to improve the Li/SE interface.^[159,162]

The Li/SE interface issues can also be addressed by chemical modification or coating of a buffer layer on the electrode or electrode/electrolyte interface (see Figure 16). The Li metal anode interface can be stabilized by forming an artificial SEI layer or a surface buffer layer, to reduce the interfacial impedance and mitigate the unnecessary side reactions to enhance the cycling efficiency of the cell. Many groups have investigated solving this issue by different approaches, such as implementing buffer layers like Au,^[164]

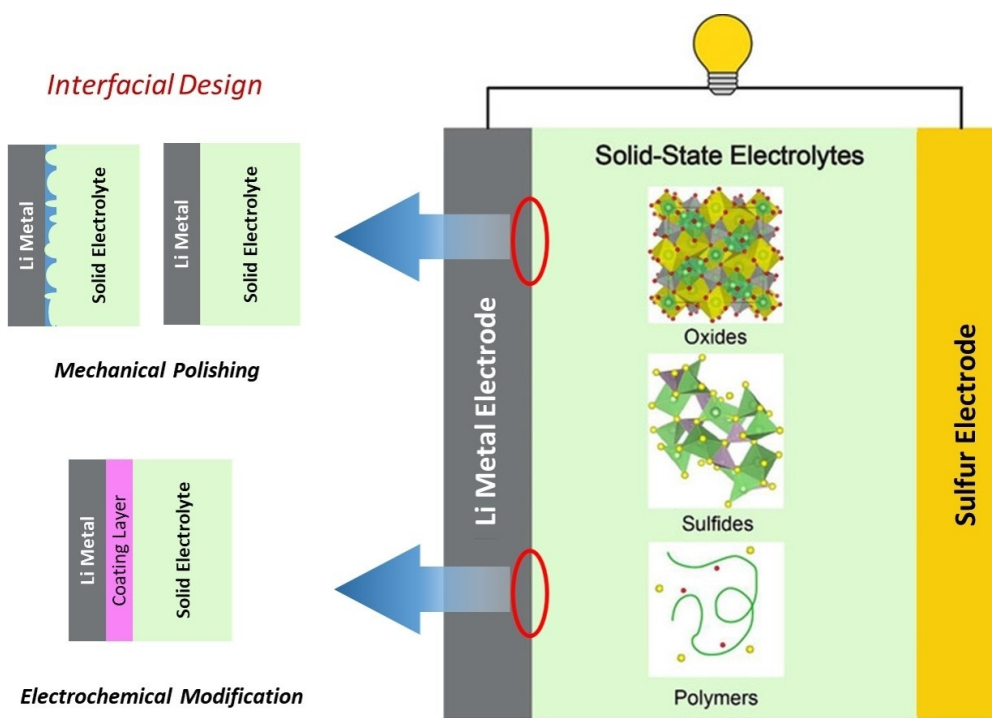


Figure 16. Schematic illustration of the solid-state LSB. Mechanical polishing and electrochemical modification can overcome Li/SE interface issues. Reproduced (adapted) with permission from Ref. [163]. Copyright (2021) The Authors. *Electrochemical Science Advances* published by Wiley-VCH GmbH.

Al_2O_3 coating by atomic layer deposition (ALD),^[165] and sputter-coated Au layer films,^[166,167] in order to relieve the contact problem between the SE and the electrodes. This kind of surface coating materials are highly conductive for lithium ions, and chemically/electrochemically stable with electrode materials such as lithium and sulfur. Another method to optimize the Li/SE interface is to apply lithium-rich compounds e.g., lithium salts, LiF or Li_3PO_4 . They serve as an ideal surface coating layer because of their good chemical stability. Fan *et al.* coated the lithium metal anode with LiF-rich SEI layer, which successfully suppressed Li-dendrite growth, while the low electronic conductivity of the LiF blocked side reactions between SE and Li metal. Therefore, an increase of current density was possible.^[168]

To stabilize the interface between lithium anode and SEs in LSBs, several approaches were reported. The use of lithium alloy can reduce the reducibility and activity of metallic lithium. A strategy to enhance the surface wettability for the SE toward Li metal could be to deposit an ultrathin intermediate such as: Al_2O_3 , ZnO, Ge, Si or Al on garnets. These intermediates will form continuous and conformal interfaces: LiAl, LiZn, LiGe and LiSi alloys. Among them, Li–In alloy is the most widely used.^[169]

Another beneficial approach is to introduce some drops of an IL or liquid electrolytes to the Li/SE interface, reducing the interfacial resistance, by increasing the wettability between the Li metal and the SE. For LGPS a 1.0 M LiTFSI-Pyr₁₃TFSI was employed as an interface modifier. The overall interface stability was improved by forming an in-situ SEI layer and the interfacial resistance could be reduced by a factor of 20.

Additionally, the cyclability in symmetrical Li metal cells was enhanced.^[170]

3.3. Composite solid-state electrolytes

Organic polymer and ISEs are not ideal candidates for LSBs. ISEs possess relatively high ionic conductivity but suffer from instability with lithium and high interfacial resistance. Polymer electrolytes obtain a high flexibility and provide good contact with electrodes, but they do suffer from low ionic conductivity.^[136] A combination of both materials is one solution to mitigate these issues. The addition of plasticizers can enhance the ionic conductivity of SPEs, although by sacrificing mechanical strength. However, composite polymer electrolytes (CSEs) with solid state fillers have been extensively studied.^[171–174] There are basically two broad categories of fillers, the (i) inert (non-ionically conductive) fillers and the (ii) Li-ionically conductive fillers:

- (i) Various inorganic oxides have been applied as inert fillers for PEO-based electrolytes, such as Al_2O_3 ,^[171] SiO_2 ^[172] and TiO_2 .^[175] The oxide nanoparticles act like a Lewis acid and can associate with the oxygen atoms in PEO chains, reducing the crystallization of the PEO and weakening the interaction between polymer and Li-ions, which leads to an improved ion conduction. Liang *et al.*^[173] employed SiO_2 as filler. The LSB showed reversible discharge capacity of approximately 800 mAh g^{-1} after 25 cycles. Judez *et al.*^[114,176] employed Al_2O_3 . However, the cell showed low discharge capacity of only 300 mAh g^{-1} , even though Al_2O_3

has outstanding interfacial property towards Li anode. In this case, they assume that LiPSs generated during the discharge process could diffuse away from the cathode and anchor on the Al_2O_3 surface. These LiPSs could not be further reduced to the final discharge product Li_2S because of loss of electrical contact, resulting in a large capacity loss. To solve this issue Li-ion conducting glass-ceramic was adopted.^[171]

- (ii) Li-ionically conductive fillers can additionally offer extra Li-ion diffusion routes by lowering the crystallinity of the polymer matrix. Li ion can be transported not only along polymer chains but also through conductive fillers in CPEs. There are three different transport pathways of Li in CPEs:^[177] (a) Li ion migration along polymer chains, (b) Li ion transport between interfacial regions of fillers and polymers, (c) Li ion migration across Li-ion conductive filler, as visualized in Figure 17.

An example for composite electrolyte applied in LSB is displayed in Figure 18. The CSE consists of $\text{Al}^{3+}/\text{Nb}^{5+}$ co-doped cubic LLZO and $\text{P}(\text{EO})_6/\text{LiClO}_4$ polymer and was investigated by Tao et al.^[174] The active S materials were embedded into porous

carbon foam decorated by LLZO nanoparticles ($\text{S}@\text{LLZO}@\text{C}$), in order to increase the ion/electron conductivity of sulfur cathode. As-prepared all-solid-state LSB shows acceptable specific capacity ($> 900 \text{ mAh g}^{-1}$ at 37°C) and high Coulombic Efficiency (close to 100%). The LLZO nanoparticles not only act as ion-conductive fillers but also as interfacial stabilizer to reduce the interfacial resistance.^[174]

The ionic conductivity of CPEs can be influenced by many factors: (i) the amount of Li-ion conductive fillers. Li et al. investigated $\text{PEO}/\text{LiClO}_4$ -based CPE with each 15 wt% and 30 wt% Al^{3+} and Nb^{5+} co-doped LLZO. They deduced that by increasing the weight ratio of LLZO in CPE, the ionic conductivity decreased. From this research we can conclude that the addition of solid-state fillers can promote the ionic conductivity of polymer electrolytes to some extent. However, it is important to carefully regulate the quantity in the polymer. Too many fillers may lead to aggregation, phase separation and will finally deteriorate the performances of CPEs.^[178] (ii) The structure design of fillers can relieve the aggregation of particles allowing a high weight ratio of filler in a polymer matrix. This would lead to a better mechanical property and preferable thermal stability of CPE, as shown in the example of

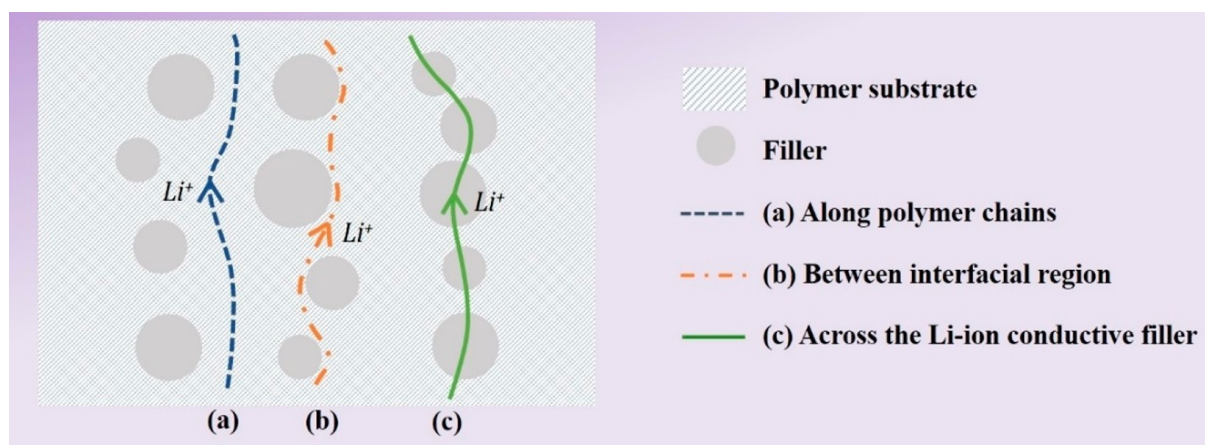


Figure 17. Schematic of Li-ion transport in CPEs. The transporting pathways are a) along polymer chains, b) between interfacial regions of fillers and polymers, and c) across the Li-ion conductive fillers. Reproduced with permission from Ref. [177]. Copyright (2020) American Chemical Society.

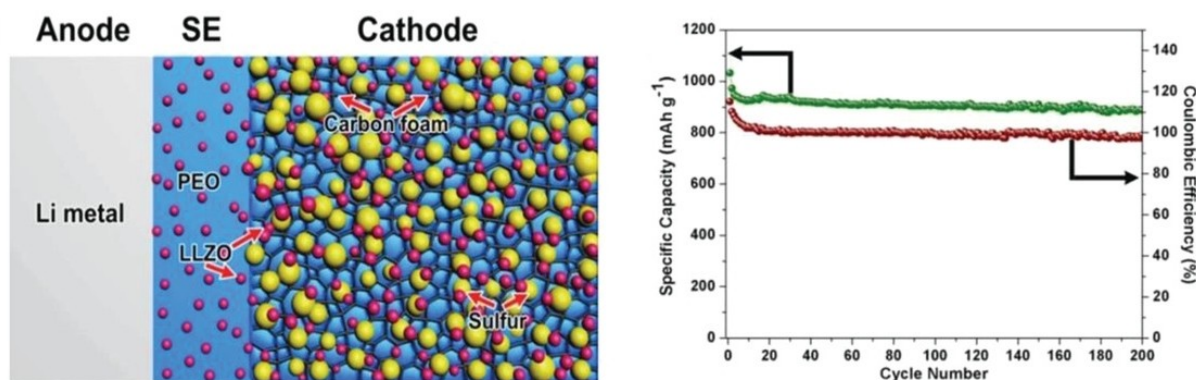


Figure 18. Schematic illustration of an all-solid-state LSB based on LLZO nanostructures. The cycling performance and Coulombic Efficiency of the S-LLZO-C cathode with a current density of 0.05 mA cm^{-2} at 37°C . Reproduced with permission from Ref. [174]. Copyright (2017) American Chemical Society.

an 3D nanostructured LLZO framework in PEO polymer.^[179] (iii) Other characteristics pertaining to fillers such as particle size, chemical composition impact the conductivity of CPE.^[180]

However, it should be noted that the specific capacity of S cathode in all-solid-state battery using CSEs is still lower and its rate and cycling performance are poor due to the larger interfacial resistance between S cathode and SCEs as well as severe volume expansion. Therefore, integrated S cathode/CSEs architectures with lower interfacial resistance and highly stable structure should be studied in future research.^[181] Recently Zhong *et al.* reported a fully integrated LSB. The battery has no distinct interfaces between SPE and anode/cathode. The mobility of EO segments is controlled by cross-linking degree of the polymer electrolyte framework. As the LiPS dissolves in the membrane there is no shuttling, resulting in batteries with high capacity (1,428 mA h g⁻¹) and high retention.^[182]

4. Conclusion and Perspectives

Continual technological advancements have increased the worldwide reliance on energy sources elevating the demand for the next step in the development of sustainable energy storage systems. The electrochemical and non-electrochemical features of sulfur make it a very promising cathode material for the next-generation batteries which go beyond the intercalation mechanism. However, the complex chemistry controlling the function of LSBs necessitates a holistic approach encompassing all the cell components. The results obtained through the past years indicate that the challenges encountered in the development of LSBs can be effectively resolved yet there is a noticeable difference between results obtained in coin cells and the performances in pouch cells.

The commercialization of lithium sulfur technology depends on its capability to outperform the traditional lithium-ion intercalation systems. In the conversion chemistry of LSBs, the electrolyte plays an arguably more important role in the achievement of superior specific energies with respect to LIBs. Type of electrolyte, composition, amount, and interactions with lithium metal are all factors that must be considered in the development of viable electrolytes for LSBs.

The management of the polysulfides shuttle is currently the most challenging obstacle. Currently, two different approaches are utilized: (i) restrain the LiPSs solubility limiting the solvating power of the electrolyte solution or, in contrast, (ii) boost the solubility of LiPSs to minimize the E/S ratio. Although remarkable achievements are already reported in the scientific literature, unfortunately, most of the approaches regarding liquid electrolytes, ignore the use of realistic parameters. Volumes of electrolyte in the order of 5 μ L, or lower, per mg of sulfur in the cathode are essential for practical LSBs but E/S ratio $> 15 \mu\text{L mg}^{-1}$ are widely reported in many publications.^[183]

In the case of SPEs, the optimization of PEO-based electrolyte is still ongoing with challenges, such as the inferior thermal stability of PEO-based SPEs needs to be addressed. Thus, the structure optimization of PEO-based matrixes should be the focus of future research. For instance, cross-linked network

polymer matrixes with abundant EO units enable superior mechanical strengths. The development of hyperbranched or block PEO-based polymer matrixes with the low crystallinity or amorphous property that can render enhanced ion-conducting abilities should also be considered.

The shuttle effect of LiPSs can be effectively restricted in inorganic electrolyte based LSBs. However, the large ceramic electrolyte/electrode interfacial resistance appears to be the main disadvantage leading to the large polarization. Utilization of composite electrolytes with special structures containing inorganic electrolyte and SPEs (LLZO nanoparticle was filled in PEO) in LSBs can effectively suppress the shuttle effect of sulfur and improve interfacial contact simultaneously. However, it is significant to develop high-voltage-resistant polymer matrix or improve the electrochemical window of polymer electrolyte using ISEs to broaden the CSE application in LSBs. Furthermore, integrated S cathode/SCEs architectures with lower interfacial resistance and highly stable structure should be examined.

These aspects currently hinder an effective scale-up, and thus the commercial viability of LSBs technology. The complexity of the Li-S chemistry still requires an understanding of the underlying mechanisms of the system, providing a foundation for rational design.

Finally, to bridge the gap, approaches which combine scientific research and industry are required to fulfil the potential of LSB technology.

Acknowledgements

The authors at HIU acknowledge the support from the Helmholtz Association. G.D.D. acknowledges Sapienza University of Rome for the financial support in the framework of "Progetti per Avvio alla Ricerca 2021" (project number: AR12117A86D341B9) and Erasmus + Programme – Student Mobility for Traineeship – Unipharm-Graduates Project 2020/2021 for the travel grant allowing the traineeship at Helmholtz Institute Ulm. H.A. acknowledges the Hong Kong Quantum AI Lab (HKQAI) for supporting his fellowship. Open Access funding enabled and organized by Projekt DEAL.

Conflict of Interest

The authors declare no conflict of interest.

Keywords: electrolyte · interface · interphase · lithium-sulfur battery

- [1] Y. Zhao, O. Pohl, A. I. Bhatt, G. E. Collis, P. J. Mahon, T. R  ther, A. F. Hollenkamp, *Sustain. Chem.* **2021**, *2*, 167–205.
- [2] D. Larcher, J. M. Tarascon, *Nat. Chem.* **2015**, *7*, 19–29.
- [3] F. Wu, J. Maier, Y. Yu, *Chem. Soc. Rev.* **2020**, *49*, 1569–1614.
- [4] U. S. Geological Survey, *Mineral Commodity Summaries 2022*, **2022**.
- [5] European Commission, *Critical Raw Materials Resilience: Charting a Path towards Greater Security and Sustainability*, **2020**.
- [6] H. Danuta, U. Juliusz, *US3043896A*, **1962**.

- [7] M. L. B. Rao, *US3413154A*, 1968.
- [8] D. A. Nole, V. Moss, *US3532543A*, 1970.
- [9] G. Zhou, *Design, Fabrication and Electrochemical Performance of Nanostructured Carbon Based Materials for High-Energy Lithium-Sulfur Batteries*, Springer, Singapore, 2017.
- [10] R. Xu, I. Belharouak, X. Zhang, R. Chamoun, C. Yu, Y. Ren, A. Nie, R. Shahbazian-Yassar, J. Lu, J. C. M. Li, K. Amine, *ACS Appl. Mater. Interfaces* **2014**, *6*, 21938–21945.
- [11] H. Chu, H. Noh, Y. K. J. Kim, S. Yuk, J. J. H. Lee, J. J. H. Lee, H. Kwack, Y. K. J. Kim, D. K. Yang, H. T. Kim, *Nat. Commun.* **2019**, *10*, 188.
- [12] M. Shaibani, M. S. Mirshekarloo, R. Singh, C. D. Easton, M. C. Dilusha Cooray, N. Eshraghi, T. Abendroth, S. Dörfler, H. Althues, S. Kaskel, A. F. Hollenkamp, M. R. Hill, M. Majumder, *Sci. Adv.* **2020**, *6*, eaay2757.
- [13] S. H. Chung, C. H. Chang, A. Manthiram, *Adv. Funct. Mater.* **2018**, *28*, 1801188.
- [14] J. Wang, S. Yi, J. Liu, S. Sun, Y. Liu, D. Yang, K. Xi, G. Gao, A. Abdelkader, W. Yan, S. Ding, R. V. Kumar, *ACS Nano* **2020**, *14*, 9819–9831.
- [15] H. Park, O. Tamwattana, J. Kim, S. Buakeaw, R. Hongtong, B. Kim, P. Khomein, G. Liu, N. Meethong, K. Kang, *Adv. Energy Mater.* **2021**, *11*, 2003039.
- [16] R. Fang, S. Zhao, Z. Sun, D. W. Wang, H. M. Cheng, F. Li, *Adv. Mater.* **2017**, *29*, 1606823.
- [17] G. Ma, Z. Wen, M. Wu, C. Shen, Q. Wang, J. Jin, X. Wu, *Chem. Commun.* **2014**, *50*, 14209–14212.
- [18] C. Yan, X. Q. Zhang, J. Q. Huang, Q. Liu, Q. Zhang, *Trends Chem.* **2019**, *1*, 693–704.
- [19] Y. Yao, X. Zhang, B. Li, C. Yan, P. Chen, J. Huang, Q. Zhang, *InfoMat* **2020**, *2*, 379–388.
- [20] B. Liu, R. Fang, D. Xie, W. Zhang, H. Huang, Y. Xia, X. Wang, X. Xia, J. Tu, *Energy Environ. Mater.* **2018**, *1*, 196–208.
- [21] J. Tan, D. Liu, X. Xu, L. Mai, *Nanoscale* **2017**, *9*, 19001–19016.
- [22] Q. He, A. T. S. Freiberg, M. U. M. Patel, S. Qian, H. A. Gasteiger, *J. Electrochem. Soc.* **2020**, *167*, 080508.
- [23] Q. Zou, Y. C. Lu, *J. Phys. Chem. Lett.* **2016**, *7*, 1518–1525.
- [24] G. Minton, in *Lithium-Sulfur Batteries*. (Eds.: M. Wild, G. J. Offer), John Wiley & Sons, Ltd, 2019, pp. 3–32.
- [25] W. Ren, W. Ma, S. Zhang, B. Tang, *Energy Storage Mater.* **2019**, *23*, 707–732.
- [26] C. Liang, N. J. Dudney, J. Y. Howe, *Chem. Mater.* **2009**, *21*, 4724–4730.
- [27] W. Yang, W. Yang, A. Song, G. Sun, G. Shao, *Nanoscale* **2018**, *10*, 816–824.
- [28] C. Zhao, L. Liu, H. Zhao, A. Krall, Z. Wen, J. Chen, P. Hurley, J. Jiang, Y. Li, *Nanoscale* **2014**, *6*, 882–888.
- [29] M. Yang, D. Shi, X. Sun, Y. Li, Z. Liang, L. Zhang, Y. Shao, Y. Wu, X. Hao, *J. Mater. Chem. A* **2020**, *8*, 296–304.
- [30] J. Song, T. Xu, M. L. Gordin, P. Zhu, D. Lv, Y. B. Jiang, Y. Chen, Y. Duan, D. Wang, *Adv. Funct. Mater.* **2014**, *24*, 1243–1250.
- [31] H. J. Peng, T. Z. Hou, Q. Zhang, J. Q. Huang, X. B. Cheng, M. Q. Guo, Z. Yuan, L. Y. He, F. Wei, *Adv. Mater. Interfaces* **2014**, *1*, 1400227.
- [32] T. Z. Hou, X. Chen, H. J. Peng, J. Q. Huang, B. Q. Li, Q. Zhang, B. Li, *Small* **2016**, *12*, 3283–3291.
- [33] Z. A. Ghazi, X. He, A. M. Khattak, N. A. Khan, B. Liang, A. Iqbal, J. Wang, H. Sin, L. Li, Z. Tang, *Adv. Mater.* **2017**, *29*, 1606817.
- [34] S. Bai, X. Liu, K. Zhu, S. Wu, H. Zhou, *Nat. Energy* **2016**, *1*, 16094.
- [35] J. Balach, T. Jaumann, M. Klose, S. Oswald, J. Eckert, L. Giebeler, *Adv. Funct. Mater.* **2015**, *25*, 5285–5291.
- [36] D. Zhu, T. Long, B. Xu, Y. Zhao, H. Hong, R. Liu, F. Meng, J. Liu, *J. Energy Chem.* **2021**, *57*, 41–60.
- [37] H. Sakaebe, in *Encycl. Appl. Electrochem.* (Eds.: G. Kreysa, K. Ota, R. F. Savinell), Springer New York, New York, 2014, pp. 1197–1201.
- [38] Q. He, Y. Gorlin, M. U. M. Patel, H. A. Gasteiger, Y.-C. Lu, *J. Electrochem. Soc.* **2018**, *165*, A4027–A4033.
- [39] T. Yim, M. S. Park, J. S. Yu, K. Kim, K. Y. Im, J. H. Kim, G. Jeong, Y. N. Jo, S. G. Woo, K. S. Kang, I. Lee, Y. J. Kim, *Electrochim. Acta* **2013**, *107*, 454–460.
- [40] L. Carbone, T. Coneglian, M. Gobet, S. Munoz, M. Devany, S. Greenbaum, J. Hassoun, *J. Power Sources* **2018**, *377*, 26–35.
- [41] A. Benítez, D. Di Lecce, Á. Caballero, J. Morales, E. Rodríguez-Castellón, J. Hassoun, *J. Power Sources* **2018**, *397*, 102–112.
- [42] H. Ryu, H. Ahn, K. Kim, J. Ahn, K. Cho, T. Nam, J. Kim, G. Cho, *J. Power Sources* **2006**, *163*, 201–206.
- [43] J. Gao, M. A. Lowe, Y. Kiya, H. D. Abruña, *J. Phys. Chem. C* **2011**, *115*, 25132–25137.
- [44] S. S. Zhang, *J. Power Sources* **2013**, *231*, 153–162.
- [45] R. Younesi, G. M. Veith, P. Johansson, K. Edström, T. Vegge, *Energy Environ. Sci.* **2015**, *8*, 1905–1922.
- [46] L. Kong, L. Yin, F. Xu, J. Bian, H. Yuan, Z. Lu, Y. Zhao, *J. Energy Chem.* **2021**, *55*, 80–91.
- [47] S. Urbonaite, T. Poux, P. Novák, *Adv. Energy Mater.* **2015**, *5*, 1500118.
- [48] C. Yang, P. Li, J. Yu, L. Da Zhao, L. Kong, *Energy* **2020**, *201*, 117718.
- [49] M. Zhao, B. Q. Li, H. J. Peng, H. Yuan, J. Y. Wei, J. Q. Huang, *Angew. Chem. Int. Ed.* **2020**, *59*, 12636–12652; *Angew. Chem.* **2020**, *132*, 12736–12753.
- [50] Q. Jin, X. Qi, F. Yang, R. Jiang, Y. Xie, L. Qie, Y. Huang, *Energy Storage Mater.* **2021**, *38*, 255–261.
- [51] X.-B. Cheng, J.-Q. Huang, Q. Zhang, *J. Electrochem. Soc.* **2018**, *165*, A6058–A6072.
- [52] C. Shen, J. Xie, M. Zhang, P. Andrei, M. Hendrickson, E. J. Plichta, J. P. Zheng, *Electrochim. Acta* **2017**, *248*, 90–97.
- [53] L. Cheng, L. A. Curtiss, K. R. Zavadil, A. A. Gewirth, Y. Shao, K. G. Gallagher, *ACS Energy Lett.* **2016**, *1*, 503–509.
- [54] G. Ma, Z. Wen, J. Jin, M. Wu, G. Zhang, X. Wu, J. Zhang, *Solid State Ionics* **2014**, *262*, 174–178.
- [55] J. W. Park, K. Yamauchi, E. Takashima, N. Tachikawa, K. Ueno, K. Dokko, M. Watanabe, *J. Phys. Chem. C* **2013**, *117*, 4431–4440.
- [56] J. W. Park, K. Ueno, N. Tachikawa, K. Dokko, M. Watanabe, *J. Phys. Chem. C* **2013**, *117*, 20531–20541.
- [57] K. Ueno, J. W. Park, A. Yamazaki, T. Mandai, N. Tachikawa, K. Dokko, M. Watanabe, *J. Phys. Chem. C* **2013**, *117*, 20509–20516.
- [58] T. Mandai, K. Yoshida, K. Ueno, K. Dokko, M. Watanabe, *Phys. Chem. Chem. Phys.* **2014**, *16*, 8761–8772.
- [59] K. Dokko, N. Tachikawa, K. Yamauchi, M. Tsuchiya, A. Yamazaki, E. Takashima, J.-W. Park, K. Ueno, S. Seki, N. Serizawa, M. Watanabe, *J. Electrochem. Soc.* **2013**, *160*, A1304–A1310.
- [60] D. J. Eyckens, L. C. Henderson, *Front. Chem.* **2019**, *7*, 263.
- [61] M. Cuisinier, P. E. Cabelguen, B. D. Adams, A. Garsuch, M. Balasubramanian, L. F. Nazar, *Energy Environ. Sci.* **2014**, *7*, 2697–2705.
- [62] C. C. Su, M. He, R. Amine, K. Amine, *Angew. Chem. Int. Ed.* **2019**, *58*, 10591–10595; *Angew. Chem.* **2019**, *131*, 10701–10705.
- [63] S. Gu, R. Qian, J. Jin, Q. Wang, J. Guo, S. Zhang, S. Zhuo, Z. Wen, *Phys. Chem. Chem. Phys.* **2016**, *18*, 29293–29299.
- [64] S. Drvarič Talian, S. Jeschke, A. Vizintin, K. Pirnat, I. Arčon, G. Aquilanti, P. Johansson, R. Dominko, *Chem. Mater.* **2017**, *29*, 10037–10044.
- [65] N. Azimi, Z. Xue, I. Bloom, M. L. Gordin, D. Wang, T. Daniel, C. Takoudis, Z. Zhang, *ACS Appl. Mater. Interfaces* **2015**, *7*, 9169–9177.
- [66] M. L. Gordin, F. Dai, S. Chen, T. Xu, J. Song, D. Tang, N. Azimi, Z. Zhang, D. Wang, *ACS Appl. Mater. Interfaces* **2014**, *6*, 8006–8010.
- [67] H. Lu, Y. Yuan, K. Zhang, F. Qin, Y. Lai, Y. Liu, *J. Electrochem. Soc.* **2015**, *162*, A1460–A1465.
- [68] H. Lu, Z. Chen, Y. Yuan, H. Du, J. Wang, X. Liu, Z. Hou, K. Zhang, J. Fang, Y. Qu, *J. Electrochem. Soc.* **2019**, *166*, A2453–A2458.
- [69] L. Suo, Y. S. Hu, H. Li, M. Armand, L. Chen, *Nat. Commun.* **2013**, *4*, 1481.
- [70] E. S. Shin, K. Kim, S. H. Oh, W. Il Cho, *Chem. Commun.* **2013**, *49*, 2004–2006.
- [71] X. Cao, H. Jia, W. Xu, J.-G. Zhang, *J. Electrochem. Soc.* **2021**, *168*, 010522.
- [72] J. G. Zhang, W. Xu, J. Xiao, X. Cao, J. Liu, *Chem. Rev.* **2020**, *120*, 13312–13348.
- [73] A. Gupta, A. Bhargava, A. Manthiram, *Adv. Energy Mater.* **2019**, *9*, 1803096.
- [74] M. Baek, H. Shin, K. Char, J. W. Choi, *Adv. Mater.* **2020**, *32*, 2005022.
- [75] H. Shin, M. Baek, A. Gupta, K. Char, A. Manthiram, J. W. Choi, *Adv. Energy Mater.* **2020**, *10*, 2001456.
- [76] J.-G. Zhang, W. Xu, W. A. Henderson, *Lithium Metal Anodes and Rechargeable Lithium Metal Batteries*, Springer, Cham, 2017.
- [77] W. Liu, P. Liu, D. Mitlin, *Adv. Energy Mater.* **2020**, *10*, 2002297.
- [78] E. Markevich, G. Salitra, Y. Talyosef, F. Chesneau, D. Aurbach, *J. Electrochem. Soc.* **2017**, *164*, A6244–A6253.
- [79] C. Kensy, D. Leistenschneider, S. Wang, H. Tanaka, S. Dörfler, K. Kaneko, S. Kaskel, *Batteries & Supercaps* **2021**, *4*, 612–622.
- [80] X. Chen, H. Ji, Z. Rao, L. Yuan, Y. Shen, H. Xu, Z. Li, Y. Huang, *Adv. Energy Mater.* **2022**, *12*, 2102774.
- [81] E. Markevich, G. Salitra, A. Rosenman, Y. Talyosef, F. Chesneau, D. Aurbach, *J. Mater. Chem. A* **2015**, *3*, 19873–19883.
- [82] M. Zhao, B. Q. Li, X. Q. Zhang, J. Q. Huang, Q. Zhang, *ACS Cent. Sci.* **2020**, *6*, 1095–1104.
- [83] X. Xiong, W. Yan, C. You, Y. Zhu, Y. Chen, L. Fu, Y. Zhang, N. Yu, Y. Wu, *Front. Chem.* **2019**, *7*, 827.

- [84] Y. V. Mikhaylik, *US7354680B2*, **2008**.
- [85] S. Xiong, K. Xie, Y. Diao, X. Hong, *J. Power Sources* **2014**, *246*, 840–845.
- [86] L. Zhang, M. Ling, J. Feng, L. Mai, G. Liu, J. Guo, *Energy Storage Mater.* **2018**, *11*, 24–29.
- [87] S. S. Zhang, *Electrochim. Acta* **2012**, *70*, 344–348.
- [88] S. S. Zhang, *J. Electrochem. Soc.* **2012**, *159*, A920–A923.
- [89] S. Liu, G. R. Li, X. P. Gao, *ACS Appl. Mater. Interfaces* **2016**, *8*, 7783–7789.
- [90] W. Jia, C. Fan, L. Wang, Q. Wang, M. Zhao, A. Zhou, J. Li, *ACS Appl. Mater. Interfaces* **2016**, *8*, 15399–15405.
- [91] J. S. Kim, D. J. Yoo, J. Min, R. A. Shakoor, R. Kahraman, J. W. Choi, *ChemNanoMat* **2015**, *1*, 240–245.
- [92] H. Pan, K. S. Han, M. Vijayakumar, J. Xiao, R. Cao, J. Chen, J. Zhang, K. T. Mueller, Y. Shao, J. Liu, *ACS Appl. Mater. Interfaces* **2017**, *9*, 4290–4295.
- [93] F. Ding, W. Xu, G. L. Graff, J. Zhang, M. L. Sushko, X. Chen, Y. Shao, M. H. Engelhard, Z. Nie, J. Xiao, X. Liu, P. V. Sushko, J. Liu, J. G. Zhang, *J. Am. Chem. Soc.* **2013**, *135*, 4450–4456.
- [94] X. Ni, T. Qian, X. Liu, N. Xu, J. Liu, C. Yan, *Adv. Funct. Mater.* **2018**, *28*, 1706513.
- [95] F. Wu, J. Qian, R. Chen, J. Lu, L. Li, H. Wu, J. Chen, T. Zhao, Y. Ye, K. Amine, *ACS Appl. Mater. Interfaces* **2014**, *6*, 15542–15549.
- [96] J. Li, S. Liu, Y. Cui, S. Zhang, X. Wu, J. Xiang, M. Li, X. Wang, X. Xia, C. Gu, J. Tu, *ACS Appl. Mater. Interfaces* **2020**, *12*, 56017–56026.
- [97] Z. Lin, Z. Liu, W. Fu, N. J. Dudney, C. Liang, *Adv. Funct. Mater.* **2013**, *23*, 1064–1069.
- [98] S. Kim, Y. M. Kwon, K. Y. Cho, S. Yoon, *Electrochim. Acta* **2021**, *391*, 138927.
- [99] F. Wu, J. T. Lee, N. Nitta, H. Kim, O. Borodin, G. Yushin, *Adv. Mater.* **2015**, *27*, 101–108.
- [100] Y. X. Ren, T. S. Zhao, M. Liu, Y. K. Zeng, H. R. Jiang, *J. Power Sources* **2017**, *361*, 203–210.
- [101] Y. Wang, Y. Meng, Z. Zhang, Y. Guo, D. Xiao, *ACS Appl. Mater. Interfaces* **2021**, *13*, 16545–16557.
- [102] S. Li, H. Dai, Y. Li, C. Lai, J. Wang, F. Huo, C. Wang, *Energy Storage Mater.* **2019**, *18*, 222–228.
- [103] G. Li, Y. Gao, X. He, Q. Huang, S. Chen, S. H. Kim, D. Wang, *Nat. Commun.* **2017**, *8*, 850.
- [104] W. Guo, W. Zhang, Y. Si, D. Wang, Y. Fu, A. Manthiram, *Nat. Commun.* **2021**, *12*, 3031.
- [105] D. Kang, M. Xiao, J. P. Lemmon, *Batteries & Supercaps* **2021**, *4*, 445–455.
- [106] E. Cha, M. D. Patel, J. Park, J. Hwang, V. Prasad, K. Cho, W. Choi, *Nat. Nanotechnol.* **2018**, *13*, 337–343.
- [107] W. Wang, X. Yue, J. Meng, J. Wang, X. Wang, H. Chen, D. Shi, J. Fu, Y. Zhou, J. Chen, Z. Fu, *Energy Storage Mater.* **2019**, *18*, 414–422.
- [108] N. Akhtar, X. Sun, M. Yasir Akram, F. Zaman, W. Wang, A. Wang, L. Chen, H. Zhang, Y. Guan, Y. Huang, *J. Energy Chem.* **2020**, *52*, 310–317.
- [109] M. Barghamadi, A. S. Best, A. I. Bhatt, A. F. Hollenkamp, M. Musameh, R. J. Rees, T. R  ther, *Energy Environ. Sci.* **2014**, *7*, 3902–3920.
- [110] Y. V. Mikhaylik, J. R. Akridge, *J. Electrochem. Soc.* **2004**, *151*, A1969.
- [111] S. Li, W. Zhang, J. Zheng, M. Lv, H. Song, L. Du, *Adv. Energy Mater.* **2021**, *11*, 2000779.
- [112] F. Zheng, M. Kotobuki, S. Song, M. O. Lai, L. Lu, *J. Power Sources* **2018**, *389*, 198–213.
- [113] Z. Xue, D. He, X. Xie, *J. Mater. Chem. A* **2015**, *3*, 19218–19253.
- [114] X. Judez, H. Zhang, C. Li, G. G. Eshetu, Y. Zhang, J. A. Gonz  lez-Marcos, M. Armand, L. M. Rodr  guez-Martinez, *J. Phys. Chem. Lett.* **2017**, *8*, 3473–3477.
- [115] S. Rajendran, T. Uma, *Bull. Mater. Sci.* **2000**, *23*, 27–29.
- [116] S. Rajendran, O. Mahendran, R. Kannan, *Fuel* **2002**, *81*, 1077–1081.
- [117] M. S. Su’Ait, A. Ahmad, H. Hamzah, M. Y. A. Rahman, *J. Phys. D* **2009**, *42*, 055410.
- [118] C. Wan, C. R. Bowen, *J. Mater. Chem. A* **2017**, *5*, 3091–3128.
- [119] C. Y. Chiang, M. Jaipal Reddy, P. P. Chu, *Solid State Ionics* **2004**, *175*, 631–635.
- [120] L. N. Sim, F. C. Sentanin, A. Pawlicka, R. Yahya, A. K. Arof, *Electrochim. Acta* **2017**, *229*, 22–30.
- [121] K. M. Abraham, M. Alamgir, *J. Electrochem. Soc.* **1990**, *137*, 1657–1658.
- [122] B. Kurc, *Electrochim. Acta* **2014**, *125*, 415–420.
- [123] B. Scrosati, F. Croce, S. Panero, *J. Power Sources* **2001**, *100*, 93–100.
- [124] R. C. Agrawal, G. P. Pandey, *J. Phys. D* **2008**, *41*, 223001.
- [125] Y. X. Song, Y. Shi, J. Wan, S. Y. Lang, X. C. Hu, H. J. Yan, B. Liu, Y. G. Guo, R. Wen, L. J. Wan, *Energy Environ. Sci.* **2019**, *12*, 2496–2506.
- [126] X. Yang, K. R. Adair, X. Gao, X. Sun, *Energy Environ. Sci.* **2021**, *14*, 643–671.
- [127] R. Fang, H. Xu, B. Xu, X. Li, Y. Li, J. B. Goodenough, *Adv. Funct. Mater.* **2021**, *31*, 2001812.
- [128] H. Marceau, C. S. Kim, A. Paolella, S. Ladouceur, M. Lagac  , M. Chaker, A. Vijh, A. Guerfi, C. M. Julien, A. Mauger, M. Armand, P. Hovington, K. Zaghbi, *J. Power Sources* **2016**, *319*, 247–254.
- [129] F. Croce, G. B. Appetecchi, L. Persi, B. Scrosati, *Nat. Lett.* **1998**, *394*, 456–458.
- [130] V. Di Noto, S. Lavina, G. A. Giffin, E. Negro, B. Scrosati, *Electrochim. Acta* **2011**, *57*, 4–13.
- [131] H. Zhang, C. Liu, L. Zheng, F. Xu, W. Feng, H. Li, X. Huang, M. Armand, J. Nie, Z. Zhou, *Electrochim. Acta* **2014**, *133*, 529–538.
- [132] X. Judez, H. Zhang, C. Li, J. A. Gonz  lez-Marcos, Z. Zhou, M. Armand, L. M. Rodr  guez-Martinez, *J. Phys. Chem. Lett.* **2017**, *8*, 1956–1960.
- [133] G. G. Eshetu, X. Judez, C. Li, M. Martinez-Iba  ez, I. Gracia, O. Bondarchuk, J. Carrasco, L. M. Rodr  guez-Martinez, H. Zhang, M. Armand, *J. Am. Chem. Soc.* **2018**, *140*, 9921–9933.
- [134] H. Zhang, U. Oteo, X. Judez, G. G. Eshetu, M. Martinez-Iba  ez, J. Carrasco, C. Li, M. Armand, *Joule* **2019**, *3*, 1689–1702.
- [135] H. Zhang, X. Judez, A. Santiago, M. Martinez-Iba  ez, M.   . Mu  oz-M  rquez, J. Carrasco, C. Li, G. G. Eshetu, M. Armand, *Adv. Energy Mater.* **2019**, *9*, 1900763.
- [136] W. Liu, D. Lin, J. Sun, G. Zhou, Y. Cui, *ACS Nano* **2016**, *10*, 11407–11413.
- [137] L. Yue, J. Ma, J. Zhang, J. Zhao, S. Dong, Z. Liu, G. Cui, L. Chen, *Energy Storage Mater.* **2016**, *5*, 139–164.
- [138] Z. Zhang, D. Sherlock, R. West, R. West, K. Amine, L. J. Lyons, *Macromolecules* **2003**, *36*, 9176–9180.
- [139] L. Chen, L. Fan, *Energy Storage Mater.* **2018**, *15*, 37–45.
- [140] Y. Hao, S. Wang, F. Xu, Y. Liu, N. Feng, P. He, H. Zhou, *ACS Appl. Mater. Interfaces* **2017**, *9*, 3375–33739.
- [141] X. Huang, C. Liu, Y. Lu, T. Xiu, J. Jin, M. E. Badding, Z. Wen, *J. Power Sources* **2018**, *382*, 190–197.
- [142] M. M. U. Din, R. Murugan, *Electrochem. Commun.* **2018**, *93*, 109–113.
- [143] M. Nagao, A. Hayashi, M. Tatsumisago, *Electrochim. Acta* **2011**, *56*, 6055–6059.
- [144] Q. Zhang, D. Cao, Y. Ma, A. Natan, P. Aurora, H. Zhu, *Adv. Mater.* **2019**, *31*, 1901131, 1901131.
- [145] N. Kamaya, K. Homma, Y. Yamakawa, M. Hirayama, R. Kanno, M. Yonemura, T. Kamiyama, Y. Kato, S. Hama, K. Kawamoto, A. Mitsui, *Nat. Mater.* **2011**, *10*, 682–686.
- [146] Y. Mo, S. P. Ong, G. Ceder, *Chem. Mater.* **2012**, *24*, 15–17.
- [147] A. Pradel, M. Ribes, *Solid State Ionics* **1986**, *18–19*, 351–355.
- [148] H. Muramatsu, A. Hayashi, T. Ohtomo, S. Hama, M. Tatsumisago, *Solid State Ionics* **2011**, *182*, 116–119.
- [149] T. Kobayashi, Y. Imade, D. Shishihara, K. Homma, M. Nagao, R. Watanabe, T. Yokoi, A. Yamada, R. Kanno, T. Tatsumi, *J. Power Sources* **2008**, *182*, 621–625.
- [150] M. Nagao, Y. Imade, H. Narisawa, T. Kobayashi, R. Watanabe, T. Yokoi, T. Tatsumi, R. Kanno, *J. Power Sources* **2013**, *222*, 237–242.
- [151] K. B. Hatzell, X. C. Chen, C. L. Cobb, N. P. Dasgupta, M. B. Dixit, L. E. Marbella, M. T. McDowell, P. P. Mukherjee, A. Verma, V. Viswanathan, A. S. Westover, W. G. Zeier, *ACS Energy Lett.* **2020**, *5*, 922–934.
- [152] Q. Tu, L. Barroso-Luque, T. Shi, G. Ceder, *Cell Reports Phys. Sci.* **2020**, *1*, 100106.
- [153] S. Wang, J. Wang, J. Liu, H. Song, Y. Liu, P. Wang, P. He, J. Xu, H. Zhou, *J. Mater. Chem. A* **2018**, *6*, 21248–21254.
- [154] X. Fu, T. Wang, W. Shen, M. Jiang, Y. Wang, Q. Dai, D. Wang, Z. Qiu, Y. Zhang, K. Deng, Q. Zeng, N. Zhao, X. Guo, Z. Liu, J. Liu, Z. Peng, *Adv. Mater.* **2020**, *32*, 2000575.
- [155] A. Sharafi, E. Kazyak, A. L. Davis, S. Yu, T. Thompson, D. J. Siegel, N. P. Dasgupta, J. Sakamoto, *Chem. Mater.* **2017**, *29*, 7961–7968.
- [156] S. Hao, H. Zhang, W. Yao, J. Lin, *J. Power Sources* **2018**, *393*, 128–134.
- [157] Y. Li, B. Xu, H. Xu, H. Duan, X. L  , S. Xin, W. Zhou, L. Xue, G. Fu, A. Manthiram, J. B. Goodenough, *Angew. Chem. Int. Ed.* **2017**, *56*, 753–756; *Angew. Chem.* **2017**, *129*, 771–774.
- [158] L. Cheng, W. Chen, M. Kunz, K. Persson, N. Tamura, G. Chen, M. Doeff, *ACS Appl. Mater. Interfaces* **2015**, *7*, 2073–2081.
- [159] L. Cheng, J. S. Park, H. Hou, V. Zorba, G. Chen, T. Richardson, J. Cabana, R. Russo, M. Doeff, *J. Mater. Chem. A* **2014**, *2*, 172–181.
- [160] Y. Gu, W. W. Wang, J. W. He, S. Tang, H. Y. Xu, J. W. Yan, Q. H. Wu, X. B. Lian, M. Sen Zheng, Q. F. Dong, B. W. Mao, *ChemElectroChem* **2019**, *6*, 181–188.
- [161] Y. Gu, W. W. Wang, Y. J. Li, Q. H. Wu, S. Tang, J. W. Yan, M. Sen Zheng, D. Y. Wu, C. H. Fan, W. Q. Hu, Z. Bin Chen, Y. Fang, Q. H. Zhang, Q. F. Dong, B. W. Mao, *Nat. Commun.* **2018**, *9*, 1339.

- [162] A. Sharafi, S. Yu, M. Naguib, M. Lee, C. Ma, H. M. Meyer, J. Nanda, M. Chi, D. J. Siegel, J. Sakamoto, *J. Mater. Chem. A* **2017**, *5*, 13475–13487.
- [163] Y. Choo, Y. Hwa, E. J. Cairns, *Electrochem. Sci. Adv.* **2021**, e2100154.
- [164] K. K. Fu, Y. Gong, B. Liu, Y. Zhu, S. Xu, Y. Yao, W. Luo, C. Wang, S. D. Lacey, J. Dai, Y. Chen, Y. Mo, E. Wachsman, L. Hu, *Sci. Adv.* **2017**, *3*, e1601659.
- [165] X. Han, Y. Gong, K. Fu, X. He, G. T. Hitz, J. Dai, A. Pearce, B. Liu, H. Wang, G. Rubloff, Y. Mo, V. Thangadurai, E. D. Wachsman, L. Hu, *Nat. Mater.* **2017**, *16*, 572–579.
- [166] S. Chen, J. Zhang, L. Nie, X. Hu, Y. Huang, Y. Yu, W. Liu, *Adv. Mater.* **2021**, *33*, 2002325.
- [167] C. L. Tsai, V. Roddatis, C. V. Chandran, Q. Ma, S. Uhlenbruck, M. Bram, P. Heitjans, O. Guillon, *ACS Appl. Mater. Interfaces* **2016**, *8*, 10617–10626.
- [168] X. Fan, X. Ji, F. Han, J. Yue, J. Chen, L. Chen, T. Deng, J. Jiang, C. Wang, *Sci. Adv.* **2018**, *4*, eaau9245.
- [169] C. J. Nen, R. A. Huggins, *Mat. Res. Bull.* **1980**, *15*, 1225–1234.
- [170] E. Umeshbabu, B. Zheng, J. Zhu, H. Wang, Y. Li, Y. Yang, *ACS Appl. Mater. Interfaces* **2019**, *11*, 18436–18447.
- [171] X. Judez, G. G. Eshetu, I. Gracia, P. López-Aranguren, J. A. González-Marcos, M. Armand, L. M. Rodríguez-Martinez, H. Zhang, C. Li, *ChemElectroChem* **2019**, *6*, 326–330.
- [172] P. M. Shanthi, P. J. Hanumantha, T. Albuquerque, B. Gattu, P. N. Kumta, *ACS Appl. Energ. Mater.* **2018**, *1*, 483–494.
- [173] X. Liang, Z. Wen, Y. Liu, H. Zhang, L. Huang, J. Jin, *J. Power Sources* **2011**, *196*, 3655–3658.
- [174] X. Tao, Y. Liu, W. Liu, G. Zhou, J. Zhao, D. Lin, C. Zu, O. Sheng, W. Zhang, H. W. Lee, Y. Cui, *Nano Lett.* **2017**, *17*, 2967–2972.
- [175] J. H. Shin, K. W. Kim, H. J. Ahn, J. H. Ahn, *Mater. Sci. Eng. B* **2002**, *95*, 148–156.
- [176] X. Judez, M. Piszcz, E. Coya, C. Li, I. Aldalur, U. Oteo, Y. Zhang, W. Zhang, L. M. Rodríguez-Martinez, H. Zhang, M. Armand, *Solid State Ionics* **2018**, *318*, 95–101.
- [177] H. Pan, Z. Cheng, P. He, H. Zhou, *Energy Fuels* **2020**, *34*, 11942–11961.
- [178] X. Li, D. Wang, H. Wang, H. Yan, Z. Gong, Y. Yang, *ACS Appl. Mater. Interfaces* **2019**, *11*, 22745–22753.
- [179] J. Bae, Y. Li, F. Zhao, X. Zhou, Y. Ding, G. Yu, *Energy Storage Mater.* **2018**, *15*, 46–52.
- [180] B. Kumar, L. G. Scanlon, R. J. Spry, *J. Power Sources* **2001**, *96*, 337–342.
- [181] S. Li, S. Q. Zhang, L. Shen, Q. Liu, J. Bin Ma, W. Lv, Y. B. He, Q. H. Yang, *Adv. Sci.* **2020**, *7*, 1903088.
- [182] L. Zhong, S. Wang, M. Xiao, W. Liu, D. Han, Z. Li, J. Qin, Y. Li, S. Zhang, S. Huang, Y. Meng, *Energy Storage Mater.* **2021**, *41*, 563–570.
- [183] S. Gu, C. Sun, D. Xu, Y. Lu, J. Jin, Z. Wen, *Electrochem. Energy Rev.* **2018**, *1*, 599–624.

Manuscript received: February 28, 2022

Revised manuscript received: April 17, 2022

Accepted manuscript online: April 26, 2022

Version of record online: May 18, 2022